Biological identification and localization of uncyclized xanthommatin, a key intermediate in ommochrome biosynthesis: an *in vitro-in vivo* study

Florent Figon[1]*, Thibaut Munsch[2], Cécile Croix[3], Marie-Claude Viaud-Massuard[3], Arnaud Lanoue[2], and Jérôme Casas[1]

From the [1]Institut de Recherche sur la Biologie de l'Insecte, UMR CNRS 7261, Université de Tours, 37200 Tours, France; [2]Biomolécules et Biotechnologies Végétales, EA 2106, Université de Tours, 37200 Tours, France; [3]Génétique, Immunothérapie, Chimie et Cancer, UMR CNRS 7292, Université de Tours, 37200 Tours, France

Running title: *Biological identification of uncyclized xanthommatin*

*To whom correspondence should be addressed: Florent Figon: Institut de Recherche sur la Biologie de l'Insecte, UMR CNRS 7261, Université de Tours, 37200 Tours, France; florent.figon@univ-tours.fr; Tel. +33 (0)2 47 36 69 81; Fax. +33 (0)2 47 36 69 66.

Keywords: Biosynthesis, color change, high-performance liquid chromatography (HPLC), insect pigment, mass spectrometry (MS), ommochromasome, ommochrome, subcellular organelle, ultraviolet-visible spectroscopy (UV-Vis spectroscopy), xanthommatin

ABSTRACT

Ommatins are widespread ommochrome pigments mediating important functions in invertebrates. While the early biogenetic steps of ommatins are well known, how their pyrido[3,2-*a*]phenoxazinone chromophore is formed and modified *in vivo* remains an unanswered question. In this study, we combined organic synthesis, analytical chemistry and organelle purification to address this issue. We analyzed the metabolites of the tryptophan→ommochrome pathway produced both *in vitro* and *in vivo*. We synthesized xanthommatin, the best-known ommatin, by oxidizing 3-hydroxykynurenine *in vitro* and we analytically characterized the products. We followed the thermal reactivity of synthesized ommatins in acidified methanol to screen for labile and altered compounds. We finally reinvestigated the ommochromes of housefly eyes by purifying and extracting the ommochrome-producing organelles called ommochromasomes. We found that the *in vitro* oxidative condensation of 3-hydroxykynurenine produces a mixture of ommatins, which readily undergo thermal reactions overtime. Our results suggest that the formation of decarboxylated ommatins might be regulated *in vivo*, while the methoxylation of ommatins, previously reported in biological extracts, are most likely always artifactitious. For the first time, we identified both *in vitro* and *in vivo* the elusive intermediate between 3-hydroxykynurenine and ommatins as being uncyclized xanthommatin. We hence confirm that ommatins are mainly biosynthesized by first the homodimerization of 3-hydroxykynurenine to the aminophenoxazinone uncyclized xanthommatin, and then an intramolecular cyclization to form the pyridine ring. We finally discuss the implication of the newly discovered uncyclized xanthommatin as a branching metabolite in the biosynthesis of ommochromes, particularly of ommins in cephalopods.

Ommochromes are widespread phenoxazinone-based pigments of invertebrates. They act as light filters in compound eyes and determine the integumental coloration of a large range of invertebrates (1). Ommochromes are also of particular interest for applied sciences as their scaffold has been used to design antitumor agents (2) and, very recently, to manufacture color changing electrochromic devices (3). The two major classes of natural ommochromes are the well-known yellow-to-red ommatins and the less-studied purple ommins, which putatively contain a supplemental phenothiazine ring. The large biological diversity of ommochromes arises from their oxidation, reduction, esterification, decarboxylation, connection with the sulfur metabolism (1), and, as recently proposed, their putative methylation (4).

The early steps of the biosynthesis of ommochromes in invertebrates cover the oxidation of tryptophan into kynurenines (Scheme 1) (1). These oxidative steps are

homologous to the kynurenine pathway of vertebrates. They involve two main enzymes, the cytosolic tryptophan 2,3-dioxygenase and the mitochondria-bound kynurenine 3-monooxygenase. The latter catalyzes the formation of 3-hydoxykynurenine, which is the currently accepted direct precursor of all known ommochromes. The catabolic pathway of tryptophan then diverges from vertebrates because invertebrates lack the glutarate pathway (5). 3-Hydroxykynurenine is the starting point of the late steps of the tryptophan→ommochrome pathway of invertebrates.

Ommochromes are produced within specialized intracellular membrane-bound organelles called ommochromasomes (Scheme 1) (1). It is hypothesized that the precursors of ommochromes, particularly 3-hydroxykynurenine, are incorporated within ommochromasomes by transmembrane transporters of the ABC family, namely White and Scarlet (6). Ommatins are easily synthesized *in vitro* by the oxidative condensation of 3-hydroxykynurenine, which is predicted to form an intermediary 3-hydroxykynurenine dimer called uncyclized xanthommatin (1, 7–10). It has long been suggested that the oxidative dimerization of 3-hydroxykynurenine also occurs *in vivo*, within ommochromasomes, to produce ommochromes (Scheme 1) (1, 7, 9). Alternatively, the condensation of *ortho*-aminophenols with xanthurenic acid has been proposed to form the pyrido[3,2-*a*]phenoxazinone chromophore of ommatins (Scheme 1) (4, 5). Which of these two possible pathways occurs *in vivo* is still unknown. Uncyclized xanthommatin was predicted *in vivo* by quantum calculations (9), putatively identified in the *in vitro* oxidation of 3-hydroxykynurenine (8) and speculated in biological extracts (11), but never formerly extracted and characterized. Finding uncyclized xanthommatin *in vivo* would be a major step in characterizing the actual biosynthetic pathway of ommochromes because only the dimerization of 3-hydroxykynurenine, not its condensation with xanthurenic acid, could account for the formation of uncyclized xanthommatin. Furthermore, whether an enzyme of the phenoxazinone synthase class is involved in the formation of ommochromes, how decarboxylated xanthommatin is biosynthesized and how the phenothiazine chromophore of ommins is related to 3-hydroxykynurenine are still key questions in the biosynthesis of ommochromes (1).

Deciphering the late steps of the biosynthetic pathway of ommochromes requires the characterization of metabolites *in vivo*. However, biological ommochromes are difficult compounds to analyze by NMR spectroscopy owing to their poor solubility in most conventional solvents (12–14), as well as to their degradability in dimethylsulfoxide (pers. obs., F. Figon). Classical photochemical studies performed photo-catalyzed methylation of extracted ommochromes by acidified methanol to produce derivative compounds (12, 15–17). Methylated ommochromes were then characterized by NMR and absorbance spectroscopies to infer the structure of the related biological ommochromes. However, photosensitive and labile metabolites, such as uncyclized xanthommatin, proved to be difficult to characterize using this method (11, 18). It is only recently that mass spectrometry (MS) has been used to help elucidating the structure of both known and unknown ommochromes from biological extracts (4, 19, 20). Yet, evidence for common and compound-specific fragmentation patterns of ommochromes are scarce (4). Together with the seldom use of synthesized ommochromes, this lack of analytical data accounts for the very little progress made since four decades to unravel the biological diversity of ommochromes. A more in-depth and exhaustive analysis of synthesized ommochromes by mass spectrometry is therefore needed to elucidate the structure of new ommochromes (1).

Photochemical studies demonstrated that ommatins are photosensitive. Upon light radiations in acidified methanol, they readily undergo methylations, methoxylations and decarboxylations (1, 17). However, their thermal stability in acidified methanol in darkness is unknown. Still, several studies reported numerous unknown ommochromes by incubating tissues in acidified methanol for several hours at room temperature and in some cases in darkness (4, 18, 21). Differentiating the biological origin of ommochromes from their artifactitious formation in extraction solvents is therefore needed before attempting any conclusion on the biodiversity of ommochromes and the related biosynthetic pathways *in Natura*.

To address the issue of potential artifactitious methoxylations and decarboxylations arising during extractions, we tested the effect of incubating synthesized ommatins in conditions mimicking classical

biological extractions. We constructed an analytical dataset of obtained ommatins by a combination of absorption, mass and tandem mass spectroscopies after separation by liquid chromatography. Based on this dataset, we could elucidate the structure of three artifactitious methoxylated ommatins with strong confidence. We then followed the kinetics of ommatins in acidified methanol in darkness and we demonstrated that xanthommatin was readily altered by methoxilations. By using our analytical tools and a newly developed extraction protocol that avoids artifacts, we reinvestigated the biological content in ommatins of housefly eyes. We also purified the ommochromasomes from housefly eyes and compared their ommochrome-related metabolites with crude extracts of housefly eyes. We could identify xanthommatin, decarboxylated xanthommatin and, most importantly, uncyclized xanthommatin with strong confidence in ommochromasomes. We finally discuss the formation of uncyclized xanthommatin as a potential key branching step in the biosynthesis of ommochromes.

Results

UPLC-DAD-MS/MS structural elucidation of synthesized xanthommatin and its in vitro *derivatives*

Since xanthommatin is commercially unavailable, we first achieved its *in vitro* synthesized by oxidative condensation of 3-hydroxykynurenine under anoxia as previously reported (22). The synthesized product was solubilized in methanol acidified with 0.5 % HCl (MeOH-HCl) and analyzed by Liquid Chromatography (LC) coupled to Diode-Array Detection (DAD) and Mass Spectrometry (MS) (Fig. 1). The product was solubilized extemporaneously to avoid any chemical degradation before LC-DAD-MS analyses (Fig. 1*A, B*). Chromatograms showed two main peaks corresponding to xanthommatin (retention time [RT]: 11.8 min, $[M+H]^+$ at *m/z* 424) and decarboxylated xanthommatin (RT: 9.1 min, $[M+H]^+$ at *m/*z 380) (Table 1). Two co-eluting peaks were present in trace amounts at RT 8.5 and 11.9 min and were associated to $[M+H]^+$ at *m/*z 460 and $[M+H]^+$ at *m/*z 504, respectively. The detailed analysis of this sample enabled the detection of a small peak at RT 6.7 min ($[M+H]^+$ at *m/*z 443) with its corresponding chromatogram at 430 nm (Fig. 1*A*). A detailed analysis of this particular compound is presented further in the text.

With the aim to disentangle the biosynthetic from the artifactitious origin of ommatin-related compounds in biological samples, the chemical stability of synthesized ommatins was first assessed by a 24h-long-incubation in MeOH-HCl at 20 °C in darkness (Fig. 1*C, D*) in order to identify potential post-extraction produced artefacts. The comparative analysis of Fig. 1*A, B* (2 minutes in MeOH-HCl) and Fig. 1*C, D* (24 h later) highlights different sets of peaks which appeared or disappeared over the 24 h of samples storage. Three major newly formed compounds were observed at RT 10.1, 12.6 and 13 min corresponding to $[M+H]^+$ at *m/*z 394, 438 and 452, respectively. We compared the UV and MS spectral characteristics of these compounds with those of xanthommatin and decarboxylated xanthommatin. Absorbance spectra of the five compounds revealed strong similarities, particularly in the visible region (> 400 nm, Figure 2*A*) suggesting that these three newly formed molecules shared their chromophores with xanthommatin and decarboxylated xanthommatin. Mass spectra of the five compounds also showed strong similarities (Figure 2*B*). They all experienced an in-source neutral loss of -17 *m/z* ($-NH_3$) and formed a double-charged molecular ion $[M+2H]^{2+}$. 452 and 394 m/z-associated compounds typically lost 14 units more than xanthommatin and decarboxylated xanthommatin, respectively, during in-source fragmentation. Additionally, their double-charged fragmentations were 7 units higher than for xanthommatin and decarboxylated xanthommatin (= 14/2; Figure 2*B*). Overall, gains of 14 *m/z* in the newly formed compounds compared to xanthommatin and decarboxylated xanthommatin suggested methylation reactions occurring in acidic methanol.

To gain further insight into the structure of those five compounds, we subjected the main $[M+H]^+$ to MS/MS fragmentation and compared it with previously reported fragmentation patterns of kynurenine, 3-hydroxykynurenine, xanthommatin and decarboxylated xanthommatin (4, 20, 23, 24) (http://metlin.scripps.edu, METLIN ID: 365). In these molecules, the main ionization site is the amine function of the amino-acid branch, which is also the most susceptible to fragmentation. For both xanthommatin and decarboxylated xanthommatin, we observed similar patterns of fragmentation of the amino-acid branch with three neutral losses

corresponding to -NH_3 (-17 *m/z*), -CH_5O_2N (-63 *m/z*) and -$C_2H_3O_2N$ (-73 *m/z*) (Table 1). Those fragmentations have been reported for these two ommatins (4, 20), as well as for kynurenines (23), indicating that they are typical of compounds with a kynurenine-like amino-acid chain. Additionally, two neutral losses corresponding to -CO_2 (-44 *m/z*) and -CH_2O_2 (-46 *m/z*) were observed only for xanthommatin (Figure 2*C*) due to the presence of the carboxyl function on the pyridine ring (Figure 2*D*). The MS/MS signatures of xanthommatin and decarboxylated xanthommatin were used to assign the structures of the three newly formed molecules. The fragmentation of $[M+H]^+$ 394 *m/z* showed neutral losses corresponding to -NH_3 (-17 *m/z*), -$C_2H_7O_2N$ (-77 = -63 -14 *m/z*) and -$C_3H_5O_2N$ (-87 = -73 -14 *m/z*) on the amino-acid branch. These results strongly indicated that, in the 394 *m/z*-associated compound, the carboxyl function of the amino-acid branch was methoxylated (α^{11} position). Consequently, this compound was assigned to decarboxylated α^{11}-methoxy-xanthommatin (Figure 2*C*). Those conclusions are in accordance with the similar absorbance spectra of decarboxylated α^{11}-methoxy-xanthommatin and decarboxylated xanthommatin (Figure 2*A*), as the amino-acid branch was unlikely to act on near-UV and visible wavelength absorptions of the chromophore. The fragmentation of $[M+H]^+$ 438 *m/z* showed the xanthommatin-like neutral losses, -NH_3 (-17 *m/z*), -CH_5O_2N (-63 *m/z*) and -$C_2H_3O_2N$ (-73 *m/z*), highlighting that this compound shared the same unaltered amino-acid branch with xanthommatin. However, this compound experienced the neutral loss -$C_2H_4O_2$ (-60 = -46 -14 *m/z*) on the pyridine ring instead of -CH_2O_2 (-46 *m/z*) (Figure 2*C*), which strongly indicated a methoxylation on the pyrido-carboxyl group (α^3 position). This is in accordance with the associated absorbance spectrum being different from that of xanthommatin, which has a carboxylated chromophore (Figure 2*A*). Hence, we proposed that this compound was α^3-methoxy-xanthommatin (Figure 2*D*). The 452 *m/z*-associated compound showed neutral losses corresponding to -NH_3 (-17 *m/z*), -$C_2H_7O_2N$ (-77 *m/z*) and -$C_3H_5O_2N$ (-87 *m/z*) on the amino-acid branch and -$C_2H_4O_2$ (-60 *m/z*) on the pyridine ring, which strongly indicated methoxylations on both pyridine ring and amino-acid branch in positions α^3 and α^{11}, respectively. This is in accordance with the associated absorbance spectrum being similar to that of α^3-methoxy-xanthommatin, which has a methoxylated chromophore. Thus, we proposed this compound to be α^3,α^{11}-dimethoxy-xanthommatin (Figure 2*D*).

Using the same DAD-MS combination approaches, we annotated other ommatin-like compounds produced during *in vitro* synthesis and after incubation in MeOH-HCl (Table 1). The 504 and 460 *m/z*-associated compounds differed from xanthommatin and decarboxylated xanthommatin by 80 Da, respectively. The associated double-charged ions $[M+2H]^{2+}$ and $[M-CH_2O_2+2H]^{2+}$ accordingly differed by 40 *m/z* from those of xanthommatin and decarboxylated xanthommatin, respectively. Their absorbance spectra were identical to the two ommatins. Their MS and MS/MS spectra revealed identical losses to xanthommatin and decarboxylated xanthommatin: -NH_3 (-17 *m/z*), -CH_2O_2 (-46 *m/z*), -CH_5O_2N (-63 *m/z*) and -$C_2H_3O_2N$ (-73 *m/z*). Furthermore, the $[M+H]^+$ 504 *m/z* experienced the same MS/MS losses -$C_2H_5O_4N$ (-107 m/z) and -$C_3H_5O_4N$ (-119 *m/z*) than xanthommatin. Alternatively, the $[M+H]^+$ 504 *m/z* experienced a unique MS loss of -153 m/z that could correspond to -$C_2H_3O_5NS$ or -$C_2H_4O_5NP$ (-73 -80 *m/z*). All those results suggested that the 504 and 460 *m/z*-associated compounds were sulphate or phosphate esters of xanthommatin and decarboxylated xanthommatin, respectively. This in accordance with the use of phosphate buufer for the *in vitro* synthesis and of sulfurous acid to precipitate ommatins. To our knowledge, these two esters have never been described so far. Finally, during the incubation in MeOH-HCl, minor ommatin-like compounds (classified as ommatins based on their absorbance and the presence of double-charged ions) were formed and were associated to the 456, 470 and 484 *m/z* (Table 1). The differences of 14 units in their respective *m/z*, as well as their neutral losses in MS/MS being similar or differing by 14 units, indicated that they were methylated versions of each other. Due to their low amounts, we could not unambiguously propose a structure.

These results showed that, in storage conditions mimicking extraction procedures with MeOH-HCl, xanthommatin and its decarboxylated form are methoxylated, even in darkness. Those reactions are likely to result from solvent additions with acidified MeOH-HCl (the most efficient solvent for ommatin extraction). To further characterize the importance of those artifactitious reactions, we followed the kinetic of the five ommatins described in Figure 2*D* in MeOH-HCl at 20 °C and in darkness.

The ommatin profile is rapidly and readily modified overtime by artifactitious methoxylations in acidified methanol

Because absorbance spectra of all five considered compounds did not differ significantly and because some of them were co-eluted (Fig. 1), their detection and quantification were performed by MS/MS in multiple reaction monitoring (MRM) mode. MRM conditions were independently optimized for each compound based on the fragmentation of their amino-acid branch (Fig. S1).

The MRM signal of xanthommatin rapidly decreased overtime in a linear fashion, with a near 40 % reduction after only one day of incubation (Figure 3*A*). On the contrary, the MRM kinetics of α^3-methoxy-xanthommatin had a logarithmic-shape, sharply increasing during the first day before reaching a plateau during the two following days (Figure 3*B*). Both decarboxylated α^{11}-methoxy-xanthommatin and α^3,α^{11}-dimethoxy-xanthommatin appeared after a few hours of incubation. Their MRM signal then linearly increased overtime (Figure 3*C, E*). In parallel, the MRM signal of decarboxylated xanthommatin stayed nearly constant, with only a small increase by 1.13 % over the five first hours (Figure 3*D*). Those results further validate that xanthommatin was readily methoxylated in darkness, primarily in position α^3. A slower methoxylation on the amino-acid branch could account for the delay in the appearance of the two other methoxylated forms. The levels of decarboxylated xanthommatin did not vary much overtime although its methoxycarbonyl ester was produced (Figure 3*D, E*). This result could be explained by the concomitant and competitive slow decarboxylation of xanthommatin, a reaction that has already been described in MeOH-HCl upon light radiations (12).

Because we cannot compare MRM signal intensities of different molecules, we took benefit of their similar absorption in the visible region, especially at 414 nm (Figure 2*A*, Fig. S2), to quantify their relative amounts. Although less sensitive and less specific than MRM-based detection, the absorbance at 414 nm strongly indicated that, after only one day of incubation, one third of ommatins was methoxylated (Figure 3*F*). Most of the methoxylated ommatins accumulated during the first 24 hours (Figure 3*B*). As expected, rates of methoxylation were significantly decreased by incubating synthesized ommatins in MeOH-HCl at -20 °C (Fig. S3*A, B*). After storage of a month at -20 °C, the methoxylated ommatins represented nearly 1.2 % of ommatins (Fig. S3*C*).

To conclude, our results showed that decarboxylated xanthommatin was mostly stable in MeOH-HCl. By contrast, xanthommatin was rapidly chemically converted into methoxylated derivatives. Since, MeOH-HCl is the most efficient solvent for ommatin extraction, the conditions for extraction and analysis of ommatins from biological samples should avoid wherever possible the formation of artifactitious methoxylated ommatins.

UPLC-DAD-MS/MS structural elucidation of uncyclized xanthommatin, the labile intermediate in the synthesis of ommatins from 3-hydroxykynurenine

The *in vitro* synthesis of xanthommatin by oxidizing 3-hydroxykynurenine additionally yielded a minor compound at RT 6.7 min. It was characterized by a peak of absorbance at 430 nm and was associated to the 443 *m/z* feature (Fig. 1*A, B*). Upon solubilization in MeOH-HCl, the unidentified compound was labile and disappeared after the 24h-incubation at 20 °C in darkness (Fig. 1*C, D*). A similar 443 *m/z* feature was described two decades ago during oxidations of 3-hydroxykynurenine in various conditions (8). Based on its MS spectrum, it was assigned putatively to the 3-hydroxykynurenine dimer called uncyclized xanthommatin. However, there was a lack of analytical evidence to support its structural elucidation. No study has ever since reported the presence of uncyclized xanthommatin, either *in vitro* or *in vivo*. Because this compound could be an important biological intermediate in the formation of ommatins (8, 12), we further characterized its structure based on its chemical behavior, absorbance and fragmentation pattern.

The absorbance and MS kinetics of the unidentified synthesized compound showed that it was very labile (insets of Figure 4*A, B*). Indeed, we could not detect it after a week of storage at -20 °C anymore. This behavior resembles that of a photosensitive ommatin isolated 40 years ago from several invertebrates, which rapidly turned into xanthommatin after extraction (11). The absorbance spectrum of this unidentified compound matched very closely that of cinnabarinic acid (Figure 4*C*). This result indicated that this compound contained an

aminophenoxazinone chromophore rather than the pyrido[3,2-*a*]phenoxazinone scaffold of ommatins or the *ortho*-aminophenol core of 3-hydroxykynurenine. Furthermore, its ionization pattern revealed striking similarities with ommatins. Along with the molecular ion $[M+H]^+$ at 443 *m/z* (corresponding to MW 442 and to the formula $C_{20}H_{18}N_4O_8$), we detected the double-charged ion $[M-NH_3+2H]^{2+}$ at 213.6 *m/z* (Figure 4*D*). The $[M+H]^+$ underwent several in-source neutral losses: $-NH_3$ (-17 m/z), $-N_2H_6$ (-34 *m/z*) and $-C_2H_6O_2N_2$ (-90 *m/z*). The MS/MS pattern at collision energies (CE) of 20 eV and 30 eV revealed the same fragments along with several others. By measuring the differences in their respective *m/z*, we classified the involved fragmentation events into four types: $F_A = -NH_3$ (-17 *m/z*), $F_B = -H_2O$ (-18 *m/z*), $F_C = -CO$ (-28 *m/z*) and $F_D = -C+2H$ (-10 *m/z*) (Figure 4*E, F*). At a CE of 30 eV each type of fragmentation occurred twice (denoted F_1 and F_2; Figure 4*F*), indicating that two similar chemical structures were present in the unidentified compound. Those fragmentations were analogous to those experienced only once by the amino-acid chains of unaltered ommatins. For example, the $-NH_3$, $-CH_5O_2N$ and $-C_2H_3O_2N$ fragments of xanthommatin (Figure 2*C*) corresponded to the fragmentations F_A, $F_A+F_B+F_C$ and $F_A+F_B+F_C+F_D$, respectively.

All these characteristics strongly supported that this labile compound was the phenoxazinonic dimer of 3-hydroxykynurenine (Figure 4*G*), called uncyclized xanthommatin (1). The oxidation of an *ortho*-aminophenol, such as 3-hydroxykynurenine, by potassium ferricyanide induces its dimerization through the loss of six electrons and protons (MW_{dimer} [442] = 2x $MW_{monomer}$ [224] - 6). The lability of uncyclized xanthommatin in cold MeOH-HCl (insets of Figure 4*A, B*), as well as the formation of a major double-charged ion corresponding to that of the reduced form of xanthommatin (dihydroxanthommatin; Figure 4*G* and Fig. S4) could be explained by the spontaneous intramolecular cyclization involving the amine functions of the aminophenoxazinone core and the closest amino-acid branch (10). The presence of two kynurenine-derived amino-acid chains, which both fragment in the same way, would explain the double-fragmentation pattern (F_A followed by F_B) of the $[M+H]^+$ (Figure 4*E, F*). Therefore, we have now the tools to identify uncyclized xanthommatin in other samples, particularly biological materials.

The in vivo *localization of the metabolites from the tryptophan→ommochrome pathway*

Using our chemical and analytical knowledge of synthesized ommatins, we reinvestigated the content of housefly eyes in ommochromes and their related metabolites. We chose this species because it is known to accumulate xanthommatin and some metabolites of the kynurenine pathway in its eyes (5). However, nothing is known about decarboxylated xanthommatin and uncyclized xanthommatin because they were recently described [(1) and this study], even though the presence of uncyclized xanthommatin has been suspected (11). Furthermore, a protocol to extract and purify ommochromasomes from housefly eyes is available (25), thus we can address the question of the localization of the metabolites from the tryptophan→ommochrome pathway. Finally, we designed an extraction protocol in which all steps were performed in darkness, at low temperature and in less than half an hour. In those conditions, we were confident that artifactitious methoxylated ommatins would represent less than one percent of all ommatins and that we could still detect uncyclized xanthommatin.

Based on MRM signals, we detected in methanolic extractions of housefly eyes (called crude extracts; Figure 5*A*) the following metabolites of the tryptophan→ommochrome pathway: tryptophan, 3-hydroxykynurenine, xanthurenic acid, xanthommatin, decarboxylated xanthommatin and uncyclized xanthommatin (Figure 5*B*, Table 1). We ascertained the identification of uncyclized xanthommatin by acquiring its absorbance, MS and MS/MS spectra in biological samples. They showed the same features than synthesized uncyclized xanthommatin (Fig. S5).

We then purified ommochromasomes from housefly eyes by a combination of differential centrifugation and ultracentrifugation, and we compared the extracted compounds with those of crude extracts (Figure 5*A*). The main metabolites of ommochromasomes were xanthommatin and its decarboxylated form (Figure 5*D*), in accordance to the function of ommochromasomes as ommochrome factories (1). Based on the absorbance at 414 nm, decarboxylated xanthommatin represented 5.3 ± 0.1 % (mean ± SD, n = 5) of all ommatins detected

in extracts of ommochromasomes. In comparison, decarboxylated ommatins represented 21.5 ± 0.2 % (mean ± SD, n = 10) of all ommatins synthesized *in vitro*, a percentage four times higher than in methanolic extracts of purified ommochromasomes (Welch two sample *t*-test, t = 219.99, df = 12.499, p-value < $2.2e^{-16}$). Regarding the precursors of ommochromes in housefly eyes, we could only detect tryptophan and 3-hydroxykynurenine but not the intermediary kynurenine. Tryptophan remained undetectable in extracts of ommochromasomes (Figure 5*D*). Xanthurenic acid, the product of 3-hydroxykynurenine transamination, was particularly present in crude extracts of housefly eyes but much less in ommochromasomes relatively to 3-hydroxykynurenine (Figure 5*C* vs. Figure 5*E*). We also detected the uncyclized form of xanthommatin in ommochromasomes (Figure 5*D*). Its level was similar to the more stable xanthurenic acid and was enriched relatively to 3-hydroxykynurenine in ommochromasomes compared to crude extracts (Figure 5*C* vs. Figure 5*E*).

We detected in ommochromasomes two minor ommatin-like compounds associated to the molecular ions 500 and 456 *m/*z (Table 1), which co-eluted with xanthommatin and its decarboxylated form, respectively (Figure 5*D*). Both unknown compounds were undetectable in crude extracts of housefly eyes. Their associated *m/z* features differed from those of xanthommatin and decarboxylated xanthommatin by 76 units, respectively (Table 1). Because the isolation buffer used for ommochromasome purifications contained β-mercaptoethanol (MW 78), we tested whether those unknown ommatins could be produced by incubating synthesized ommatins with β-mercaptoethanol in a water-based buffer. We did find that 456 and 500 *m/z*-associated compounds were rapidly formed in those *in vitro* conditions and that their retention times matched those detected in ommochromasome extracts (Fig. S6). Therefore, the 456 and 500 *m/z*-associated ommatins detected in ommochromasome extracts were likely artifacts arising from the purification procedure via the addition of β-mercaptoethanol. These results further demonstrate that ommochromes are likely to be altered during extraction and purification procedures, a chemical behavior that should be controlled by using synthesized ommochromes incubated in similar conditions than biological samples.

Discussion

UPLC-DAD-MS/MS structural elucidation of new ommatins

Ommatins are difficult compounds to analyze by NMR spectroscopy (12); their structural elucidation remains therefore extremely challenging. To characterize the structure of new ommatins, we used a combination of absorption and mass spectroscopies after separation by liquid chromatography. We report here the most comprehensive analytical dataset to date of ommatins, based on their absorbance, mass and tandem mass spectra (Table 1). This dataset allowed us to elucidate with strong confidence the structure of four new ommatins, including three artifacts and one labile biological intermediate, and to propose structures for eight new other ommatins.

Unexpectedly, the mass spectra in positive mode of ommochromes proved to be highly valuable for the identification of new ommatins. In our conditions, all and only ommochromes formed a major double-charged molecular ion $[M+2H]^{2+}$, except uncyclized xanthommatin that formed $[M-NH_3+2H]^{2+}$ probably after intramolecular cyclization. Double charging during electronic ionization has been reported for phenoxazine-related compounds (26, 27). Since this structure is the backbone of all ommochromes, it might facilitate the in-source formation of double-charged species. Indeed, the presence of three to four basic amine sites in ommochromes might further enhance double charging in the electrospray source. Hence, the presence of double-charged ions in unknown samples, together with the λ_{max} presented above, might be a good indicator for the presence of ommochromes. The typical in-source fragmentation of the amino-acid chain of ommochromes ($-NH_3$, $-CH_2O_2$ and $-C_2H_3O_2N$) also brought information on the position of methoxylations by a shift of -14 *m/z* when present. Simple MS could therefore be used to gain insight into the structure of unknown ommochromes when MS/MS is not available.

Studies reporting the MS/MS spectra of ommatins demonstrated that they primarily fragment on their amino-acid chain (20) and then on the pyrido-carboxylic acid, if present (4). We confirmed those results for other ommatins and we took a step further by positioning methoxylations based on the differences in fragmentation between methoxylated ommatins

and (decarboxylated) xanthommatin. Besides, xanthommatin not only formed a 307 *m/z* fragment but also a major 305 *m/z* fragment (Figure 2*C*; Table 1). This sole fragment was used in a previous study to annotate a putative new ommochrome called (iso-)elymniommatin, an isomer of xanthommatin (4). Our results prove that we cannot distinguish (iso-)elymniommatin and xanthommatin unambiguously based on their MS/MS spectra. The use of synthesized ommatins and further experiments are thus needed to verify the existence of (iso-)elymniommatin in butterfly wings.

Absorbance spectra of ommatins were similar in the visible region but differed in the UV region. We distinguished four typical UV spectra corresponding to four chromophores: the 5-oxo-pyrido[3,2-*a*]phenoxazine-3-carboxylic acid (absorbance peaks [λ_{max}]: 234 and 442 nm; e.g. xanthommatin), the pyrido[3,2-*a*]phenoxazine-5-one (λ_{max}: 234 and 442 nm; e.g. decarboxylated xanthommatin), the 5-oxo-pyrido[3,2-*a*]phenoxazine-methoxy-3-carboxylate (λ_{max}: 217, 303 and 452 nm; e.g. α^{11}-methoxy-xanthommatin) and the aminophenoxazinone (λ_{max}: 235 and 420-450 nm; e.g. uncyclized xanthommatin). We hence demonstrate that xanthommatin and its decarboxylated form do not differ significantly in the visible region. This experimental result conflicts with theoretical calculations that found an absorbance peak at longer wavelength for xanthommatin (430 nm) compared to decarboxylated xanthommatin (410 nm) (20). The discrepancy with our results could come from the calculations made on uncharged ommatins in ref. (20), which did not match our acidic conditions nor the putative *in vivo* acidic conditions within ommochromasomes (1).

Overall, this analytical dataset will help future studies to identify known biosynthesized and artifactitious ommatins in biological samples, as well as to elucidate the structure of unknown ommatins by analyzing their absorbance and mass spectra. Furthermore, the presence of the biosynthetic intermediate uncyclized xanthommatin can now be tested in a wide variety of species.

Coping with artifactitious reactions during the extraction of ommatins

It has long been reported that ommatins are photosensitive compounds that react with acidified methanol (MeOH-HCl) upon light radiation, leading to their reduction, methylation, methoxylation, decarboxylation and deamination (1, 15–17). Nevertheless, efficient extraction procedures of ommatins from biological samples require the incubation of tissues in MeOH-HCl for several hours at room temperature (4, 18, 21). Our results demonstrate that, even in the absence of light radiation, ommatins are readily and rapidly methoxylated by thermal additions of methanol, primarily on the carboxylic acid function of the pyridine ring and secondarily on the amino-acid chain (Scheme 2). The $[M+H]^+$ 438 *m/z* of α^3-methoxy-xanthommatin identified in our study could correspond to the same $[M+H]^+$ previously reported in extracts of butterfly wings (4). Our results imply that the methoxylated ommatins described in that study arose from the extraction protocol and not from differences in the biosynthesis of ommatins between butterfly populations (4). We also show that ommatins react with other extraction buffers since we detected β-mercaptoethanol-added ommatins when synthesized ommatins were incubated in a phosphate buffer containing that reducing agent. This result emphasizes the need to control for potential artifactitious reactions when performing any extraction or purification protocol. Finally, some ommochromes prove to be highly unstable once extracted, leading to their spontaneous decay (11, 18, 28). This was particularly the case for uncyclized xanthommatin that rapidly underwent intramolecular cyclization at -20 °C (Scheme 2).

To limit artifacts and thus to identify the biosynthesized ommatins present in MeOH-HCl extracts, extraction protocols should follow the subsequent rules. First, all extraction steps involving MeOH-HCl should be performed at low temperature and in darkness. Second, the overall extraction should take less an hour and extracted ommatins should be analyzed as soon as possible. In those conditions, spontaneous decarboxylation of xanthommatin should account for less than one percent of all decarboxylated xanthommatin, methoxylated ommatins should be barely detectable and at least 70 % of uncyclized xanthommatin should be recovered. Third, if the analysis must be delayed, extracts should be stored at least at -20 °C in darkness and for less than a month to limit the formation of methoxylated forms to one percent of all ommatins. Finally, synthesized ommatins should be incubated and analyzed under similar conditions than extracted ommatins to control for artifactitious reactions.

The late steps of the tryptophan→ommochrome pathway in ommochromasomes

We used our chemical and analytical knowledge of synthesized ommatins to reevaluate the content of housefly eyes, which are known to contain xanthommatin (5). Because ommochromes are produced within specialized membrane-bound organelles (1), we purified ommochromasomes from housefly heads and compared their content in ommochrome-related compounds with crude extracts of housefly eyes.

It has long been hypothesized that precursors of ommochromes are translocated within ommochromasomes by the transmembrane ABC transporters White and Scarlet (6, 29). For the first time, we clearly demonstrate that 3-hydroxykynurenine, but not tryptophan, occurs in ommochromasome fractions underlying a 3-hydroxykynurine import into ommochromasomes. This results supports the hypothesis that 3-hydroxykynurine is transported into ommochromasomes via White and Scarlet transporters (Scheme 3).

Our results confirm that the main ommatin accumulated in ommochromasomes of housefly eyes is xanthommatin. We also show that decarboxylated xanthommatin is present in significant amounts, which cannot be solely due to the slow decarboxylation of xanthommatin in MeOH-HCl. This result indicates that both xanthommatin and its decarboxylated form are produced from 3-hydroxykynurenine within ommochromasomes (Scheme 3). However, the lower percentage of decarboxylated xanthommatin in ommochromasomes (5.3 %) relatively to that percentage in synthesized ommatins (21.5 %) indicates that the formation of xanthommatin is favored *in vivo* (Scheme 3). We discuss the biological implications of promoting the non-decarboxylative biosynthesis of ommatins below.

We also detected xanthurenic acid, the cyclized form of 3-hydroxykynurenine, in housefly eyes. Compared to 3-hydroxykynurenine, xanthurenic acid was present in minute amounts within ommochromasomes. We hypothesize that xanthurenic acid is produced within ommochromasomes via two non-exclusive pathways (Scheme 3). First, the *in situ* intramolecular cyclization of 3-hydroxykynurenine, which requires a transaminase activity in the cytosol (Scheme 3) (30). Second, the degradation of xanthommatin, which would produce 3-hydroxykynurenine and xanthurenic acid. The phenoxazinone structure of ommatins is indeed known to undergo ring-cleavage, particularly in slightly basic water-based buffers (7). Hence, traces of xanthurenic acid might either come from artifactitious degradation during the purification protocol or from biological changes in ommochromasome conditions (enzymatic activities or basification) leading to the cleavage of xanthommatin. To date, no biological pathways for the degradation of the phenoxazinone structure of ommochromes have been described. The detection of xanthurenic acid in ommochromasomes might therefore be the first step towards understanding the *in situ* catabolism of ommochromes (Scheme 3).

Experimental and computational chemists have long hypothesized that the pyrido[3,2-*a*]phenoxazinone structure of ommatins should be synthesized *in vivo* by the dimerization of 3-hydroxykynurenine and a subsequent spontaneous intramolecular cyclization (9, 31). However, the associated dimer of 3-hydroxykynurenine, called uncyclized xanthommatin, proved to be difficult to characterize and to isolate from biological samples because of its lability (11). In our study, we synthesized uncyclized xanthommatin by the oxidative condensation of 3-hydroxykynurenine with potassium ferricyanide, an oxidant known to form aminophenoxazinones from *ortho*-aminophenols (11). We used a combination of kinetics and analytical spectroscopy (DAD, MS and MS/MS) to confirm the *in vitro* and *in vivo* occurrence of uncyclized xanthommatin without NMR data. Because we detected xanthommatin, its decarboxylated form, their precursor 3-hydroxykynurenine and the intermediary uncyclized xanthommatin in *in vitro* and *in vivo* samples, we argue that the *in vitro* synthesis and the biosynthesis of ommatins proceed through a similar mechanism (Scheme 2 and Scheme 3). An alternative biosynthetic pathway for ommatins has been proposed to occur through the condensation of 3-hydroxykynurenine with xanthurenic acid (4, 5). However, our data does not support this hypothesis because xanthurenic acid, which is a stable compound unlike uncyclized xanthommatin, was present in minute amounts within ommochromasomes compared to 3-hydroxykynurenine. At the very least, our results show that xanthurenic acid is tightly linked to the ommochrome pathway and therefore cannot

be considered as a marker of a distinct biogenic pathway, as recently proposed for butterflies (4). As far as we know, there has been no experimental evidence for the formation of xanthommatin by condensing 3-hydroxykynurenine with xanthurenic acid. In conclusion, the formation of uncyclized xanthommatin by the oxidative dimerization of 3-hydroxykynurenine is likely to be the main biological route for the biosynthesis of ommatins within ommochromasomes (Scheme 3).

Whether the *in vivo* oxidative condensation of 3-hydroxykynurenine is catalyzed enzymatically remains a key question in the biogenesis of ommochromes (1). Theoretical calculations suggested that both enzymatic and non-enzymatic oxidations of 3-hydroxykynurenine would lead to the formation of the phenoxazinone uncyclized xanthommatin (9, 31). There was some evidence of a phenoxazinone synthase (PHS) activity associated to purified ommochromasomes of fruitflies (32). However, no corresponding PHS enzyme has ever been isolated nor identified in species producing ommochromes (1). PHS is not the only enzyme capable of forming aminophenoxazinones from *ortho*-aminophenols. Tyrosinase, laccase, peroxidase and catalase can also catalyze these reactions (33). Particularly, peroxidase can produce xanthommatin and its decarboxylated form from 3-hydroxykynurenine *in vitro* (8, 34–36), likely through the formation of uncyclized xanthommatin (8). This result relates to the long-known fact that insects mutated for the heme peroxidase Cardinal accumulate 3-hydroxykynurenine without forming ommochromes (37, 38). Hence, our data support the hypothesis that the biosynthesis of ommatins could be catalyzed by a relatively unspecific peroxidase such as Cardinal (Scheme 3) (38, 39), without the requirement of a specialized PHS.

Uncyclized xanthommatin, a potential branching point in the biogenesis of ommatins

The relatively recent description of decarboxylated xanthommatin in several species indicates that it is a widespread biological ommatin (1). Yet, little is known about how decarboxylation of ommatins proceeds *in vivo*. In this study, we show that decarboxylated xanthommatin is unlikely to arise solely from the artifactitious decarboxylation of xanthommatin in MeOH-HCl. The level of decarboxylated xanthommatin was lower *in vivo* than *in vitro*. We discuss three non-exclusive mechanisms for the biosynthesis of decarboxylated xanthommatin.

First, the decarboxylation of xanthommatin in water-based environments possibly accounted for the formation of decarboxylated xanthommatin. Some aromatic compounds are known to be decarboxylated by the action of water (40). As indirect supporting information, kynurenic acid, which is structurally related to xanthommatin, can be decarboxylated upon light radiations in water (41). Thus, the relative level of decarboxylated xanthommatin *in vivo* might depend on the exposure of xanthommatin to light Scheme 3). Second, enzymatic and non-enzymatic syntheses of ommatins might differ in their exact molecular steps, as proposed by quantum chemistry (9). Accordingly, the oxidation of 3-hydroxykynurenine by either potassium ferricyanide or peroxidase suggested that less decarboxylated xanthommatin was produced by peroxidase (34). Thus, the involvement of the heme peroxidase Cardinal in the biosynthesis of ommatins might lead to the natural formation of xanthommatin over its decarboxylated form. Finally, Bolognese and colleagues proposed that decarboxylation would happen by a rearrangement of protons, subsequently to the intramolecular cyclization of uncyclized xanthommatin (12). Such mechanism has been well described for the biogenesis of eumelanin monomers, in which dopaquinone cyclizes into dopachrome and then tautomerizes into either 5,6-dihydroxyindole-2-carboxylic acid (DHICA) or 5,6-dihydroxyindole (DHI) (42). Similarly to what we found for ommatins, the percentage of decarboxylated monomers (DHI) is generally lower in eumelanins produced *in vivo* than *in vitro* (43). During biological eumelanogenesis, the non-decarboxylative rearrangement of dopachrome is favored by the Zn-containing enzyme dopachrome tautomerase (DCT/Trp2) (44). Likewise, a tautomerase might catalyze the *in vivo* formation of xanthommatin from uncyclized xanthommatin (Scheme 3), thereby controlling the relative content of decarboxylated xanthommatin in ommochromasomes. Under this hypothesis, uncyclized xanthommatin would act as a branching metabolite in the biosynthesis of carboxylated and decarboxylated ommatins.

Few studies have addressed the biological function of decarboxylated xanthommatin. Its ratio to xanthommatin varies between species and

individuals (19, 20). In cephalopods, the ratio of xanthommatin to its decarboxylated form within a chromatophore has been suggested to determine its color, ranging from yellow to purple (20). However, our absorbance data do not support this hypothesis because the experimental absorbance spectrum of decarboxylated xanthommatin was not different from that of xanthommatin in the visible region. Moreover, purple colors are produced by chromophores that absorb wavelengths around 520 nm, which has not been described for any ommatin in contrast to ommins (1). Another study focusing on the quantum chemistry of pirenoxine, a xanthommatin-like drug, proposed that the carboxylic acid function present on the pyrido[3,2-*a*]phenoxazinone of pirenoxine could enhance its binding to divalent cations (45). This is coherent with the fact that ommochromasomes accumulate and store cations, such as Ca^{2+} and Mg^{2+} (46, 47). Thus, favoring xanthommatin over its decarboxylated form *in vivo* might enhance the storage of metals in ommochromasomes, as proposed for eumelanins that contain high proportions of the carboxylated monomers DHICA (48). To which extent the binding of metals modifies the physical and chemical properties of ommatins, therefore their biological roles, remains to be determined.

Uncyclized xanthommatin, a putative branching point between ommatins and ommins

Ommatins are currently the best described family of ommochromes (1). However, sulfur-based ommins are also widespread in the eyes of insects and in the epidermis of cephalopods (5). Purple ommins have higher molecular weights than ommatins and derive from 3-hydroxykynurenine and cysteine, the latter providing the sulfur to the putative phenothiazine ring of ommins (5, 49). The best-known ommin is called ommin A. It likely weighs 650 Da, which corresponds to the putative formula $C_{30}H_{27}N_5O_{10}S$ (50). A possible structure would hence be the trimer of 3-hydroxykynurenine in which one of the phenoxazine ring is replaced by phenothiazine (49). Under this hypothesis, it is unlikely that the biosynthesis of ommins is a side-branch of ommatins because in no way the pyrido[3,2-*a*]phenoxazinone could be reopen to an aminophenoxazinone (17).

Older genetic and chemical studies demonstrated that ommins and ommatins share common biosynthetic pathways, particularly the kynurenine pathway (5). Thus, there should be an intermediary metabolite functioning as a branching point in-between ommins and ommatins. According to the proposed structure of ommin A, this branching metabolite might well be the dimer of 3-hydroxykynurenine called uncyclized xanthommatin. Hence, the biosynthesis of ommins would first proceed by the dimerization of 3-hydroxykynurenine into uncyclized xanthommatin, then by the stabilization of its amino-acid chain to avoid a spontaneous intramolecular cyclization and finally by the condensation with a sulfur-containing compound derived from methionine. Although this mechanism is hypothetical at this stage, it might explain why *cardinal* mutants of insects, which lack the heme peroxidase Cardinal, do not produce ommatins or ommins but accumulate 3-hydroxykynurenine (37, 38). Thus, the branching metabolite between ommatins and ommins should be downstream of 3-hydroxykynurenine, a role that might be played by uncyclized xanthommatin.

Linzen proposed more than forty years ago that the ratio of xanthommatin to ommins could depend on the level of methionine-derived precursors (5). Such model of a branching metabolite with subsequent anabolic fluxes relying on the availability of sulfur-based precursors has been successfully used for melanogenesis (51, 52). There, the so-called casing model of melanins explains the successive formation of sulfur-based pheomelanins and eumelanins within a single melanosome rather well (53). Interestingly, the chromatophores of cephalopods change their ommochrome-based color from yellow to purple during their lifetime (54). Because no ommatins and no ommins are known to produce purple and yellow colors, respectively, we assume that the chromatophores of cephalopods synthesize those two types of ommochromes sequentially. Such changes in the metabolism of ommochromes in a single cell could be explained by a gradual increase in sulfur-based precursors of ommins within ommochromasomes. This uptake of sulfur-based precursors might be regulated by specific transporters in the membrane of ommochromasomes, as proposed for silkworms and red flour beetles (55). In cephalopods, after the formation of uncyclized xanthommatin, biosynthetic pathways would shift from producing ommatins towards ommins by using sulfur-based precursors predominantly, thereby

changing the color of a single chromatophore from yellow to purple (54).

Experimental Procedures

Insects

Houseflies (*Musca domestica*) were obtained at the pupal stage from Kreca. After hatching, houseflies were either directly processed for ommochromasome purification or stored at -20 °C for ommochrome extraction.

Reagents

Sodium dihydrogen phosphate, sodium hydrogen phosphate, L-kynurenine (≥ 98 %), 3-hydroxy-D,L-kynurenine, Triton X-100, tris(hydroxymethyl)aminomethane (Tris), potassium ferricyanide, magnesium chloride, potassium chloride, potassium pentoxide and cinnabarinic acid (≥ 98 %) were purchased from Sigma-Aldrich. Methanol, potassium chloride and hydrochloric acid (37 %) were purchased from Carlo Erba reagents. Nycodenz® was purchased from Axis Shield. L-tryptophan (≥ 99 %) and xanthurenic acid (≥ 96 %) were purchased from Acros Organics. Sucrose (99 %) and sulfurous acid (≥ 6 % SO_2) were purchased from Alfa Aesar. β-Mercaptoethanol was purchased from BDH Chemicals. Acetonitrile and formic acid were purchased from ThermoFischer Scientific.

In vitro *synthesis of xanthommatin*

Oxidative condensation of 3-hydroxykynurenine under anoxia

A mixture of ommatins was synthesized by oxidizing 3-hydroxy-D,L-kynurenine with potassium ferricyanide as previously described (19), with slight modifications. In a round bottom flask under argon, a solution of 44.6 mM of 3-hydroxy-D,L-kynurenine was prepared by dissolving 455 µmol (102 mg) in 10.2 mL of 0.2 M phosphate buffer at pH 7.1 (PB). In a second round bottom flask under argon, 174 mM of potassium ferricyanide (303 mg) were dissolved in 5.3 mL of PB. Both solutions were purged with argon and protected from light. The potassium ferricyanide solution was added slowly to the solution of 3-hydroxy-D,L-kynurenine. The resulted reaction mixture was stirred at room temperature for 1 h 30 in darkness. Then, 10 mL of sulfurous acid diluted four times in PB was added. The final solution was brought to 4 °C for 30 min during which red flocculants formed. The suspension was then transferred into a 50 mL centrifuge tube. The round bottom flask was rinsed with 8 mL of sulfurous acid previously diluted four times in PB. The final suspension was centrifuged for 10 min at 10 000 × g and at 4 °C. The solid was desiccated overnight under vacuum over potassium hydroxide and phosphorus pentoxide. 104 mg of a reddish brown powder was obtained and kept at 4 °C in darkness until further use.

Solubilization and analyses of synthesized ommatins

A solution of synthesized ommatins at 1 mg/mL of was made in methanol acidified with 0.5 % HCl and pre-cooled at -20 °C (MeOH-HCl). The solution was mixed for 30 s and filtered on 0.45 µm filters. All steps were performed, as much as possible, at 4 °C in darkness. The overall procedure took less than two minutes. Immediately after filtration, the solution was subjected to absorption and mass spectrometry analysis (see below). The filtered solution was then stored at 20 °C in darkness and subjected to the same analysis 24 hours later.

Ultra-Pressure Liquid Chromatography coupled to Diode-Array Detector and Electrospray Ionization Source-based Mass Spectrometer (UPLC-DAD-ESI-MS)

System

A reversed-phase ACQUITY UPLC® system coupled to a diode-array detector (DAD) and to a Xevo TQD triple quadrupole mass spectrometer (MS) equipped with an electrospray ionization source (ESI) was used (Waters, Milford, MA). Tandem mass spectrometry (MS/MS) was performed by collision-induced dissociation with argon. Data were collected and processed using MassLynx software, version 4.1 (Waters, Milford, MA).

Chromatographic conditions

Analytes were separated on a CSH™ C18 column (2.1 x 150 mm, 1.7 µm) equipped with a CSH™ C18 VanGuard™ pre-column (2.1 x 5 mm). The column temperature was set at 45 °C and the flow rate at 0.4 mL/min. The injection volume was 5 µL. The mobile phase consisted in a mixture of MilliQ water (eluent A) and acetonitrile (eluent B), both prepared with 0.1 % formic acid. The linear gradient was set from 2 % to 40 % B for 18 min.

Spectroscopic conditions

The MS continuously alternated between positive and negative modes every 20 ms. Capillary

voltage, sample cone voltage (CV) and collision energy (CE) were set at 2 000 V, 30 V and 3 eV, respectively, for MS conditions. CE was set at 30 eV for tandem MS conditions. Cone and desolvation gas flow rates were set at 30 and 1 000 L/h, respectively. Absorption spectra of analytes were continuously recorded between 200 and 500 nm with a one-nm step. Analytes were annotated and identified according to their retention times, absorbance spectra, mass spectra and tandem mass spectra (TABLE 1).

Thermal reactivity of ommatins in acidified methanol in darkness

Conditions of solubilization and incubation

Solutions (n = 5) of synthesized ommatins at 1 mg/mL were prepared in MeOH-HCl. The solutions were mixed for 30 s and filtered on 0.45 µm filters. Aliquots of 50 µL were prepared for each sample and stored at either 20 °C or -20 °C in darkness. All steps were performed, as much as possible, in darkness and at 4 °C. The overall procedure for each sample took less than two minutes. During the course of the experiment, each aliquot was analyzed only once by UPLC-ESI-MS/MS, representing a single time point for each sample.

Quantification of ommatins

Unaltered (*i.e.* xanthommatin and its decarboxylated form) and their methoxylated forms were detected and quantified by absorption and MS/MS (single reaction monitoring [MRM] mode) spectrometry. MRM conditions were optimized for each ommatin based on the following parent-to-product ion transitions: xanthommatin $[M+H]^+$ 424>361 *m/z* (CV 38 V, CE 25 eV), α^3-methoxy-xanthommatin $[M+H]^+$ 438>375 *m/z* (CV 37 V, CE 23 eV), α^3,α^{11}-dimethoxy-xanthommatin $[M+H]^+$ 452>375 *m/z* (CV 38 V, CE 25 eV), decarboxylated xanthommatin $[M+H]^+$ 380>317 *m/z* (CV 34 V, CE 28 eV) and decarboxylated α^{11}-methoxy-xanthommatin $[M+H]^+$ 394>317 *m/z* (CV 34 V, CE 28 eV). See Fig. S1 for detailed information on MS/MS optimization. Peak areas for both absorption and MRM signals were calculated by integrating chromatographic peaks with a "Mean" smoothing method (window size: ± 3 scans, number of smooths: 2). Absorbance values at 414 nm of unaltered ommatins were summed and reported as a percentage of the total absorbance of unaltered and methoxylated ommatins. The decay at -20 °C of uncyclized xanthommatin was followed by integrating both the absorbance at 430 nm and the 443 *m/z* SIR signals associated to the chromatographic peak of uncyclized xanthommatin at RT 6.7 min.

Extraction and content analysis of housefly eyes

Biological extractions

Five housefly (*M. domestica*) heads were pooled per sample (n = 5), weighted and homogenized in 1 mL MeOH-HCl with a tissue grinder (four metal balls, 300 strokes/min for 1 min). The obtained crude extracts were centrifuged for 5 min at 10 000 × g and 4 °C. The supernatants were filtered on 0.45 µm filters and immediately processed for absorption and MS analyses. All steps were performed, as much as possible, in darkness at 4 °C. The overall extraction procedure took less than 20 min.

Chromatographic profile

The chromatographic profile of housefly eyes that includes L-tryptophan, xanthurenic acid, 3-D,L-hydroxykynurenine, uncyclized xanthommatin, xanthommatin and decarboxylated xanthommatin is reported based on their optimized MRM signals. L-Tryptophan and xanthurenic acid were quantified based on their optimized MRM signals: $[M+H]^+$ 205>118 *m/z* (CV 26 V and CE 25 eV) and $[M+H]^+$ 206>132 *m/z* (CV 36 V and CE 28 eV), respectively. See Fig. S1 for detailed information on MS/MS optimization. 3-D,L-Hydroxykynurenine and uncyclized xanthommatin were quantified based on their absorption at 370 and 430 nm, respectively. L-Tryptophan, 3-D,L-hydroxykynurenine and xanthurenic acid levels were converted to molar concentrations using calibrated curves of commercial standards. Molar concentrations of uncyclized xanthommatin are reported as cinnabarinic equivalent, since both metabolites possess the same chromophore and presented similar absorbance spectra (see Figure 4*C*).

Purification and content analysis of ommochromasomes

Isolation buffers

Ommochromasomes from housefly eyes were purified as previously described (25), with some modifications. Isolation buffer (IB) was prepared with 10 mM Tris, 1 mM $MgCl_2$, 25 mM KCl and 14 mM β-mercaptoethanol in distilled water. The pH was brought to 7.0 with 1 M HCl. Isolation buffer with sucrose (IB sucrose) was prepared by adding 0.25 M sucrose to IB. IB and IB sucrose were kept at 4 °C no longer than a day to avoid β-

mercaptoethanol degradation (56). All steps of the purification procedure were performed at 4 °C.

Homogenization of housefly eyes

A total of 416 fresh housefly heads were homogenized in 12 mL of IB sucrose with a glass potter Elvehjem homogenizer. The suspension was filtered on gauze and the filtrate recovered. The potter was rinsed with 6 mL of IB sucrose, filtered and the filtrate recovered.

Differential centrifugation

The two filtrates were combined and centrifuged for 2 min at 400 × g. The supernatant was recovered. The pellet was resuspended in 6 mL IB sucrose, centrifuged for 2 min at 400 × g and the supernatant recovered. The supernatants were combined and centrifuged for 5 min at 180 × g. The supernant was recovered and centrifuged for 12 min at 10 000 × g. The obtained pellet was stored overnight at 4 °C. To limit membrane destabilization and loss of pigments by the action of detergents, the pellet was only resuspended in 12 mL IB sucrose with 30 µL Triton X-100 immediately before ultracentrifugation. The suspension containing Triton X-100 was further centrifuged for 1 min at 100 × g and the supernatant recovered.

Ultracentrifugation

The supernatant was layered onto two discontinuous gradients of (from bottom to top): 2.5 M, 2.25 M, 2 M, 1.75 M, 1.5 M, 1.25 M and 1 M sucrose in IB. The tubes were ultracentrifuged for 45 min at 175 000 × g in a Beckman LE-70 ultracentrifuge with a SW32 rotor. The obtained pellets were resuspended in 3 mL of IB sucrose, combined and layered onto a discontinuous gradient of (from bottom to top): 0.99 M, 0.83 M and 0.73 M Nycodenz® (iohexol) in IB. The tube was ultracentrifuged for 2 h 40 at 175 000 × g with a SW41Ti rotor. Purified ommochromasomes were recovered from the 0.83 M layer (corresponding density around 1.4) and centrifuged for 10 min at 23 000 × g. The obtained pellet was rinsed with IB sucrose, resuspended in 1 mL IB sucrose and fractionated into 0.1 mL aliquots. Those aliquots were centrifuged for 20 min at 12 000 × g. The supernatants were discarded and one pellet was directly processed for electron microscopy to check for the absence of membrane contaminants and other organelles, particularly mitochondria and lysosomes (FIG 5A). The remaining obtained pellets of purified ommochromasomes were stored at -20 °C until further use.

Extraction of ommochrome-related metabolites from purified ommochromasomes

Pellets (n = 5) were resuspended in 50 µL MeOH-HCl and directly subjected to UPLC-DAD-ESI-MS/MS analysis. All steps were performed, as much as possible, in darkness and at 4 °C. The overall extraction procedure took less than 2 min per sample.

Metabolic analysis of purified ommochromasomes

The chromatographic profile of purified ommochromasomes that includes L-tryptophan, xanthurenic acid, 3-D,L-hydroxykynurenine, uncyclized xanthommatin, xanthommatin, decarboxylated xanthommatin and β-mercaptoethanol-added ommatins is reported based on their optimized MRM signals. L-Tryptophan, 3-D,L-hydroxykynurenine, xanthurenic acid and uncyclized xanthommatin were quantified as described for crude extracts of housefly eyes.

Statistical analysis

Statistical analyses were performed using the R software, version 3.4.1 (www.r-project.org). Statistical threshold was set to 0.05. Statistical analyses are briefly described in the captions of Figure 3 and Figure 4, and detailed results are reported in the Supplemental File S2.

Acknowledgments: We thank Kévin Billet, Cédric Delevoye and Emmanuel Gaquerel for fruitful discussions. We are grateful to Antoine Touzé for his technical assistance and for access to the ultracentrifuge. We thank Rustem Uzbekov for providing the electron micrograph. This study formed part of the doctoral dissertation of F. F. under the supervision of J. C.

Conflict of interest: The authors declare that they have no conflicts of interest with the contents of this article.

Author contributions: F. F., A. L. and J. C. conceptualization; F. F. data curation; F. F. formal analysis; M.-C. V.-M., A. L. and J. C. funding acquisition; F. F., T. M. and C. C. investigation; F. F., T. M., C. C., A. L. and J. C. methodology; F. F., A. L. and J. C. project administration; M.-C. V.-M., A. L. and J. C. resources; J. C. supervision; F. F., A. L. and J. C. validation; F. F. visualization; F. F. and J. C. writing – original draft; F. F., T. M., C. C., M.-C. V.-M., A. L. and J. C. writing – review & editing.

References

1. Figon, F., and Casas, J. (2019) Ommochromes in invertebrates: biochemistry and cell biology. *Biological Reviews*. **94**, 156–183
2. Bolognese, A., Correale, G., Manfra, M., Lavecchia, A., Mazzoni, O., Novellino, E., Barone, V., Pani, A., Tramontano, E., La Colla, P., Murgioni, C., Serra, I., Setzu, G., and Loddo, R. (2002) Antitumor Agents. 1. Synthesis, Biological Evaluation, and Molecular Modeling of 5 *H* -Pyrido[3,2- *a*]phenoxazin-5-one, a Compound with Potent Antiproliferative Activity. *Journal of Medicinal Chemistry*. **45**, 5205–5216
3. Kumar, A., Williams, T. L., Martin, C. A., Figueroa-Navedo, A. M., and Deravi, L. F. (2018) Xanthommatin-Based Electrochromic Displays Inspired by Nature. *ACS Applied Materials & Interfaces*. 10.1021/acsami.8b14123
4. Panettieri, S., Gjinaj, E., John, G., and Lohman, D. J. (2018) Different ommochrome pigment mixtures enable sexually dimorphic Batesian mimicry in disjunct populations of the common palmfly butterfly, *Elymnias hypermnestra*. *PLOS ONE*. **13**, e0202465
5. Linzen, B. (1974) The Tryptophan → Ommochrome Pathway in Insects. in *Advances in Insect Physiology* (Treherne, J. E., Berridge, M. J., and Wigglesworth, V. B. eds), pp. 117–246, Elsevier, Academic Press, **10**, 117–246
6. Mackenzie, S. M., Howells, A. J., Cox, G. B., and Ewart, G. D. (2000) Sub-cellular localisation of the white/scarlet ABC transporter to pigment granule membranes within the compound eye of Drosophila melanogaster. *Genetica*. **108**, 239–252
7. Butenandt, A., and Schäfer, W. (1962) Ommochromes. in *Recent Progress in the Chemistry of Natural and Synthetic Colouring Matters and Related Fields*, pp. 13–33, Academic Press, New York, NY
8. Iwahashi, H., and Ishii, T. (1997) Detection of the oxidative products of 3-hydroxykynurenine using high-performance liquid chromatography–electrochemical detection–ultraviolet absorption detection–electron spin resonance spectrometry and high-performance liquid chromatography–electrochemical detection–ultraviolet absorption detection–mass spectrometry. *Journal of Chromatography A*. **773**, 23–31
9. Zhuravlev, A. V., Vetrovoy, O. V., and Savvateeva-Popova, E. V. (2018) Enzymatic and non-enzymatic pathways of kynurenines' dimerization: the molecular factors for oxidative stress development. *PLOS Computational Biology*. **14**, e1006672
10. Williams, T. L., Lopez, S. A., and Deravi, L. F. (2019) A Sustainable Route To Synthesize the Xanthommatin Biochrome via an Electro-catalyzed Oxidation of Tryptophan Metabolites. *ACS Sustainable Chem. Eng.* 10.1021/acssuschemeng.9b01144
11. Bolognese, A., and Scherillo, G. (1974) Occurrence and characterization of a labile xanthommatin precursor in some invertebrates. *Experientia*. **30**, 225–226
12. Bolognese, A., Liberatore, R., Riente, G., and Scherillo, G. (1988) Oxidation of 3-hydroxykynurenine. A reexamination. *Journal of Heterocyclic Chemistry*. **25**, 1247–1250
13. Parrilli, M., and Bolognese, A. (1992) 1H and 13C Chemical Shift Data of Some Ommochrome Models: Substituted Benzo[3,2-a]-5H-phenoxazin-5-one. *Heterocycles*. **34**, 1829
14. Crescenzi, O., Correale, G., Bolognese, A., Piscopo, V., Parrilli, M., and Barone, V. (2004) Observed and calculated ^{1}H- and ^{13}C-NMR chemical shifts of substituted 5H-pyrido[3,2-a]- and 5H-pyrido[2,3-a]phenoxazin-5-ones and of some 3H-phenoxazin-3-one derivatives. *Org. Biomol. Chem.* **2**, 1577–1581
15. Bolognese, A., Liberatore, R., and Scherillo, G. (1988) Photochemistry of ommochromes and related compounds. *Journal of Heterocyclic Chemistry*. **25**, 979–983
16. Bolognese, A., Liberatore, R., and Scherillo, G. (1988) Photochemistry of ommochromes and related compounds. Part II. *Journal of Heterocyclic Chemistry*. **25**, 1251–1254
17. Bolognese, A., and Liberatore, R. (1988) Photochemistry of ommochrome pigments. *Journal of Heterocyclic Chemistry*. **25**, 1243–1246
18. Bolognese, A., Liberatore, R., Piscitelli, C., and Scherillo, G. (1988) A Light-Sensitive Yellow Ommochrome Pigment From the House Fly. *Pigment Cell Research*. **1**, 375–378

19. Futahashi, R., Kurita, R., Mano, H., and Fukatsu, T. (2012) Redox alters yellow dragonflies into red. *Proceedings of the National Academy of Sciences*. **109**, 12626–12631
20. Williams, T. L., DiBona, C. W., Dinneen, S. R., Jones Labadie, S. F., Chu, F., and Deravi, L. F. (2016) Contributions of Phenoxazone-Based Pigments to the Structure and Function of Nanostructured Granules in Squid Chromatophores. *Langmuir*. **32**, 3754–3759
21. Riou, M., and Christidès, J.-P. (2010) Cryptic Color Change in a Crab Spider (Misumena vatia): Identification and Quantification of Precursors and Ommochrome Pigments by HPLC. *Journal of Chemical Ecology*. **36**, 412–423
22. Butenandt, A., Schiedt, U., and Biekert, E. (1954) Über Ommochrome, III. Mitteilung: Synthese des Xanthommatins. *Justus Liebigs Annalen der Chemie*. **588**, 106–116
23. Vazquez, S., Truscott, R. J. W., O'Hair, R. A. J., Weimann, A., and Sheil, M. M. (2001) A study of kynurenine fragmentation using electrospray tandem mass spectrometry. *Journal of the American Society for Mass Spectrometry*. **12**, 786–794
24. Guijas, C., Montenegro-Burke, J. R., Domingo-Almenara, X., Palermo, A., Warth, B., Hermann, G., Koellensperger, G., Huan, T., Uritboonthai, W., Aisporna, A. E., Wolan, D. W., Spilker, M. E., Benton, H. P., and Siuzdak, G. (2018) METLIN: A Technology Platform for Identifying Knowns and Unknowns. *Analytical Chemistry*. **90**, 3156–3164
25. Cölln, K., Hedemann, R., and Ojijo, E. (1981) A method for the isolation of ommochrome-containing granules from insect eyes. *Experientia*. **37**, 44–46
26. Gilbert, J. N. T., and Millard, B. J. (1969) Pharmacologically interesting compounds—I: High resolution mass spectra of phenothiazines. *Organic Mass Spectrometry*. **2**, 17–31
27. Cassan, J., Rouillard, M., Azzaro, M., and Mital, R. L. (1974) Étude d'une série de phénoxazines et d'azaphénoxazines par spectrométrie de masse. *Organic Mass Spectrometry*. **9**, 19–30
28. Bowness, J. M. (1959) A light-sensitive yellow pigment from the House-fly. *The Journal of General Physiology*. **42**, 779–792
29. Ewart, G. D., Cannell, D., Cox, G. B., and Howells, A. J. (1994) Mutational analysis of the traffic ATPase (ABC) transporters involved in uptake of eye pigment precursors in Drosophila melanogaster. Implications for structure-function relationships. *J. Biol. Chem.* **269**, 10370–10377
30. Han, Q., Beerntsen, B. T., and Li, J. (2007) The tryptophan oxidation pathway in mosquitoes with emphasis on xanthurenic acid biosynthesis. *Journal of Insect Physiology*. **53**, 254–263
31. Butenandt, A. (1957) Über Ommochrome, eine Klasse natürlicher Phenoxazon-Farbstoffe. *Angewandte Chemie*. **69**, 16–23
32. Yamamoto, M., Howells, A. J., and Ryall, R. L. (1976) The ommochrome biosynthetic pathway in Drosophila melanogaster: The head particulate phenoxazinone synthase and the developmental onset of xanthommatin synthesis. *Biochemical Genetics*. **14**, 1077–1090
33. Le Roes-Hill, M., Goodwin, C., and Burton, S. (2009) Phenoxazinone synthase: what's in a name? *Trends in Biotechnology*. **27**, 248–258
34. Ishii, T., Iwahashi, H., Sugata, R., and Kido, R. (1992) Formation of hydroxanthommatin-derived radical in the oxidation of 3-hydroxykynurenine. *Archives of biochemistry and biophysics*. **294**, 616–622
35. Vazquez, S., Garner, B., Sheil, M. M., and Truscott, R. J. (2000) Characterisation of the major autoxidation products of 3-hydroxykynurenine under physiological conditions. *Free radical research*. **32**, 11–23
36. Vogliardi, S., Bertazzo, A., Comai, S., Costa, C. V. L., Allegri, G., Seraglia, R., and Traldi, P. (2004) An investigation on the role of 3-hydroxykynurenine in pigment formation by matrix-assisted laser desorption/ionization mass spectrometry. *Rapid Communications in Mass Spectrometry*. **18**, 1413–1420
37. Howells, A. J., Summers, K. M., and Ryall, R. L. (1977) Developmental patterns of 3-hydroxykynurenine accumulation in white and various other eye color mutants of Drosophila melanogaster. *Biochem. Genet.* **15**, 1049–1059
38. Osanai-Futahashi, M., Tatematsu, K., Futahashi, R., Narukawa, J., Takasu, Y., Kayukawa, T., Shinoda, T., Ishige, T., Yajima, S., Tamura, T., Yamamoto, K., and Sezutsu, H. (2016) Positional cloning of a Bombyx pink-eyed white egg locus reveals the major role of cardinal in ommochrome synthesis. *Heredity*. **116**, 135–145

39. Liu, S.-H., Luo, J., Yang, B.-J., Wang, A.-Y., and Tang, J. (2017) *karmoisin* and *cardinal* ortholog genes participate in the ommochrome synthesis of *Nilaparvata lugens* (Hemiptera: Delphacidae). *Insect Science*. 10.1111/1744-7917.12501
40. Mundle, S. O. C., and Kluger, R. (2009) Decarboxylation via Addition of Water to a Carboxyl Group: Acid Catalysis of Pyrrole-2-Carboxylic Acid. *Journal of the American Chemical Society*. **131**, 11674–11675
41. Zelentsova, E. A., Sherin, P. S., Snytnikova, O. A., Kaptein, R., Vauthey, E., and Tsentalovich, Y. P. (2013) Photochemistry of aqueous solutions of kynurenic acid and kynurenine yellow. *Photochem. Photobiol. Sci.* **12**, 546–558
42. Borovansky, J., and Riley, P. A. (2011) *Melanins and Melanosomes: Biosynthesis, Structure, Physiological and Pathological Functions*, John Wiley & Sons, Weinheim
43. Pawelek, J. M. (1991) After Dopachrome? *Pigment Cell Research*. **4**, 53–62
44. Solano, F., JiméNez-Cervantes, C., MartíNez-Liarte, J. H., GarcíA-BorróN, J. C., Jara, J. R., and Lozano, J. A. (1996) Molecular mechanism for catalysis by a new zinc-enzyme, dopachrome tautomerase. *Biochemical Journal*. **313**, 447–453
45. Liao, J.-H., Chen, C.-S., Hu, C.-C., Chen, W.-T., Wang, S.-P., Lin, I.-L., Huang, Y.-H., Tsai, M.-H., Wu, T.-H., Huang, F.-Y., and Wu, S.-H. (2011) Ditopic Complexation of Selenite Anions or Calcium Cations by Pirenoxine: An Implication for Anti-Cataractogenesis. *Inorganic Chemistry*. **50**, 365–377
46. Gribakin, F. G., Burovina, I. V., Chesnokova, Y. G., Natochin, Y. V., Shakmatova, Y. I., Ukhanov, K. Y., and Woyke, E. (1987) Reduced magnesium content in non-pigmented eyes of the honey bee (Apis mellifera L.). *Comparative Biochemistry and Physiology Part A: Physiology*. **86**, 689–692
47. Ukhanov, K. Y. (1991) Ommochrome pigment granules: A calcium reservoir in the dipteran eyes. *Comparative Biochemistry and Physiology Part A: Physiology*. **98**, 9–16
48. Hong, L., and Simon, J. D. (2007) Current Understanding of the Binding Sites, Capacity, Affinity, and Biological Significance of Metals in Melanin. *The Journal of Physical Chemistry B*. **111**, 7938–7947
49. Needham, A. E. (1974) *The significance of zoochromes*, Zoophysiology and ecology, Springer, Berlin, Heidelburg, New York
50. Butenandt, A., and Neubert, G. (1958) Über Ommochrome, XVII. Zur Konstitution der Ommine, I. *Justus Liebigs Annalen der Chemie*. **618**, 167–173
51. Agrup, G., Hansson, C., Rorsman, H., and Rosengren, E. (1981) The effect of cysteine on oxidation of tyrosine dopa, and cysteinyldopas. *Archives of Dermatological Research*. **272**, 103–115
52. Ito, S. (2003) A Chemist's View of Melanogenesis. *Pigment Cell Research*. **16**, 230–236
53. Ito, S., and Wakamatsu, K. (2008) Chemistry of Mixed Melanogenesis—Pivotal Roles of Dopaquinone. *Photochemistry and Photobiology*. **84**, 582–592
54. Reiter, S., Hülsdunk, P., Woo, T., Lauterbach, M. A., Eberle, J. S., Akay, L. A., Longo, A., Meier-Credo, J., Kretschmer, F., Langer, J. D., Kaschube, M., and Laurent, G. (2018) Elucidating the control and development of skin patterning in cuttlefish. *Nature*. **562**, 361–366
55. Osanai-Futahashi, M., Tatematsu, K. -i., Yamamoto, K., Narukawa, J., Uchino, K., Kayukawa, T., Shinoda, T., Banno, Y., Tamura, T., and Sezutsu, H. (2012) Identification of the Bombyx Red Egg Gene Reveals Involvement of a Novel Transporter Family Gene in Late Steps of the Insect Ommochrome Biosynthesis Pathway. *Journal of Biological Chemistry*. **287**, 17706–17714
56. Stevens, R., Stevens, L., and Price, N. (1983) The stabilities of various thiol compounds used in protein purifications. *Biochemical Education*. **11**, 70

FOOTNOTES

Funding was provided by the ENS de Lyon (to F. F.).

The abbreviations used are: CE, collision energy; CV, cone voltage; DAD, diode-array detector; ESI^+, positive-mode electron spray ionization; LC, liquid chromatography; MeOH-HCl, acidified methanol with 0.5 % hydrochloric acid; MRM, multiple reaction monitoring; MS, mass spectrometry; MS/MS, tandem mass spectrometry; MW, molecular weight; *m/z*, mass-to-charge ratio; NMR, nuclear magnetic resonance; RT, retention time; SD, standard deviation; SE, standard error; SIR, single ion recording; UV, ultraviolet.

Tables

Table 1. **Analytical characteristics of ommatin-related compounds found *in vitro* or *in vivo*.**

Annotation (Formula, calculated MW)	RT (min)	Absorbance peaks	Monocharged ions (*m/z* loss)	Double-charged ions (*m/z* loss)	MS/MS fragments (*m/z* loss)
Detected in synthesized ommatins, crude extracts of housefly eyes and ommochromasome extracts					
3-Hydroxykynurenine ($C_{10}H_{12}N_2O_4$, 224.21)	1.6	231; 264; 376	224.9 $[M+H]^+$; 207.9 (-17); 161.9 (-63); 152.0 (-73)	Not detected	207.7 (-17); 161.9 (-63)
Uncyclized xanthommatin ($C_{20}H_{18}N_4O_8$, 442.38)	6.7	235; 420-450	442.9 $[M+H]^+$; 425.9 (-17); 408.8 (-34); 353.0 (-90)	213.6 $[M-17+2H]^{2+}$	425.9 (-17); 409.0 (-34); 390.9 (-52); 363.1 (-80); 353.0 (-90); 344.9 (-98); 335.1 (-108); 317.0 (-126); 307.0 (-136)
Xanthommatin ($C_{20}H_{13}N_3O_8$, 423.33)	11.8	234; 442	423.9 $[M+H]^+$; 406.8 (-17); 377.9 (-46); 350.9 (-73)	212.5 $[M+2H]^{2+}$; 189.5 (-23)	406.3 (-17; -18); 360.7 (-63); 350.8 (-73); 316.8 (-107); 304.8 (-119); 288.9 (-135)
Decarboxylated xanthommatin ($C_{19}H_{13}N_3O_6$, 379.32)	9.1	234; 442	379.9 $[M+H]^+$; 362.9 (-17); 333.9 (-46); 306.9 (-73)	190.5 $[M+2H]^{2+}$; 167.5 (-23)	362.7 (-17; -18); 333.7 (-46); 316.8 (-63); 306.8 (-73); 290.9 (-89)
Only detected in synthesized ommatins					
Xanthommatin sulphate/phosphate ester ($C_{20}H_{13}N_3O_{11}S$, 503.40; $C_{20}H_{14}N_3O_{11}P$, 503.31)	12.4	236; 445	503.9 $[M+H]^+$; 453.6 (-50); 430.5 (-73?); 379.8 (-124); 350.7 (-153)	252.5 $[M+2H]^{2+}$; 229.5 (-23)	487.0 (-17); 440.6 (-63); 430.8 (-73); 422.8 (-81); 396.5 (-107?); 384.9 (-119)
Decarboxylated xanthommatin sulphate/phosphate ester ($C_{19}H_{13}N_3O_9S$, 459.39; $C_{19}H_{14}N_3O_9P$, 459.30)	8.5	236; 443	459.8 $[M+H]^+$; 442.8 (-17); 413.8 (-46); 386.7 (-73)	230.4 $[M+2H]^{2+}$; 207.4 (-23)	442.8 (-17); 413.7 (-46); 396.8 (-63); 386.8 (-73)
Detected in synthesised ommatins incubated in MeOH-HCl in darkness					
α^3-Methoxy-xanthommatin ($C_{21}H_{15}N_3O_8$, 437.36)	12.6	217; 303; 452	437.9 $[M+H]^+$; 420.9 (-17); 391.9 (-46); 364.9 (-73)	219.4 $[M+2H]^{2+}$; 196.5 (-23)	420.7 (-17); 391.8 (-46); 374.8 (-63); 364.8 (-73); 314.8 (-123); 304.8 (-133)
α^3, α^{11}-Dimethoxy-xanthommatin ($C_{22}H_{17}N_3O_8$, 451.39)	13.0	217; 303; 452	451.9 $[M+H]^+$; 434.9 (-17); 391.9 (-60); 364.9 (-87)	226.5 $[M+2H]^{2+}$; 196.4 (-30)	434.9 (-17); 374.8 (-77); 364.9 (-87); 314.8 (-137); 304.8 (-147)
Decarboxylated α^{11}-methoxy-xanthommatin ($C_{20}H_{15}N_3O_6$, 393.35)	10.1	234; 442	393.9 $[M+H]^+$; 376.9 (-17); 333.9 (-60); 307.0 (-87)	197.6 $[M+2H]^{2+}$; 167.4 (-30)	376.7 (-17; -18); 333.8 (-60); 316.8 (-77); 306.9 (-87); 290.9 (-105)
Unknown altered xanthommatin (455)	14.4	242; 442	455.9 $[M+H]^+$	228.4 $[M+2H]^{2+}$; 205.4 (-23)	340.1 (-116); 324.6 (-131?); 295.0 (-161); 205.2 (-251)
Unknown altered methoxy-xanthommatin (469)	14.9	243; 390; 452	469.8 $[M+H]^+$	235.5 $[M+2H]^{2+}$; 212.4 (-23)	353.7 (-116); 338.8 (-131); 294.7 (-175); 204.8 (-265)
Unknown altered dimethoxy-xanthommatin (483)	15.0	242; 388; 450	484.0 $[M+H]^+$	242.5 $[M+2H]^{2+}$; 212.5 (-30)	353.9 (-130); 338.8 (-145); 294.8 (-189); 204.9 (-279)
Detected in synthesized ommatins incubated with β-mercaptoethanol in darkness and in ommochromasome extracts					
β-mercaptoethanol-added xanthommatin ($C_{22}H_{17}N_3O_9S$, 499.45)	11.7	238; 415	499.9 $[M+H]^+$; 426.8 (-73)	250.4 $[M+2H]^{2+}$; 227.5 (-23); 218.4 (-32)	482.7 (-17); 464.7 (-35)
β-mercaptoethanol-added decarboxylated xanthommatin ($C_{21}H_{17}N_3O_7S$, 455.44)	9.1	232; 412	455.9 $[M+H]^+$; 420.0 (-36); 382.8 (-73); 343.8 (-112)	228.4 $[M+2H]^{2+}$; 205.4 (-23); 196.5 (-32)	438.8 (-17); 421.0 (-35); 392.7 (-63)

Figures

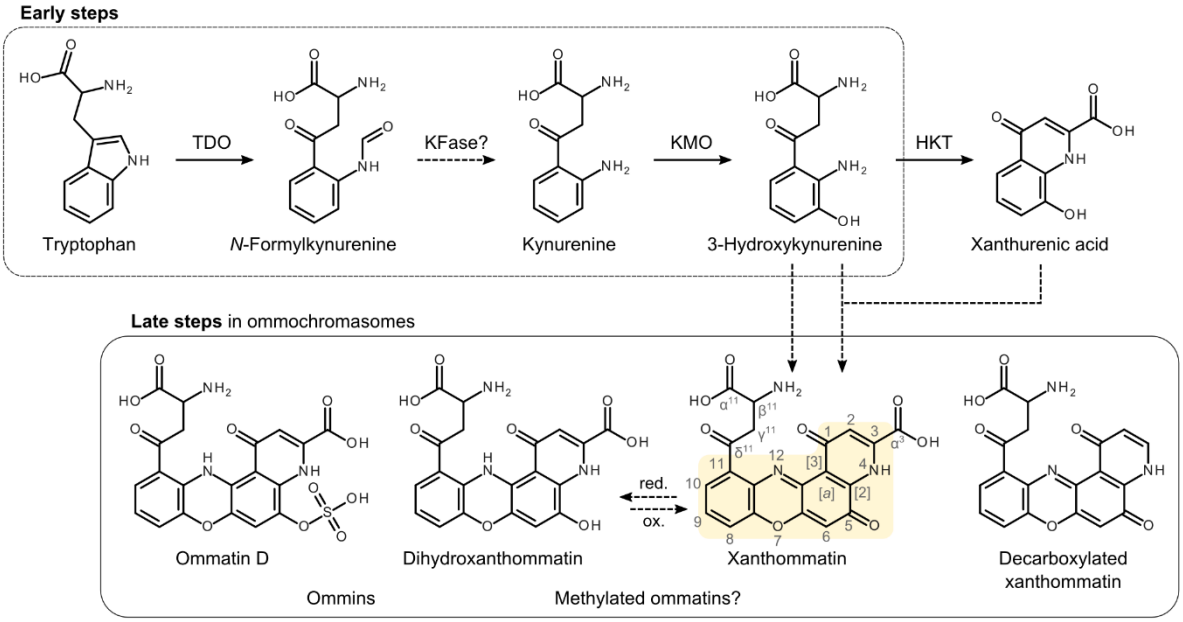

Scheme 1. **The tryptophan→ommochrome pathway of invertebrates.** Carbon numbering used in this study is shown in grey fonts for xanthommatin and is similar for all ommatins. Dashed arrows, reactions for which we lack clear evidence of an enzymatic activity; they can be either putative or spontaneous. HKT, 3-hydroxykynurenine transaminase. KFase, kynurenine formamidase. KMO, kynurenine 3-monooxygenase. TDO, tryptophan 2,3-dioxygenase.

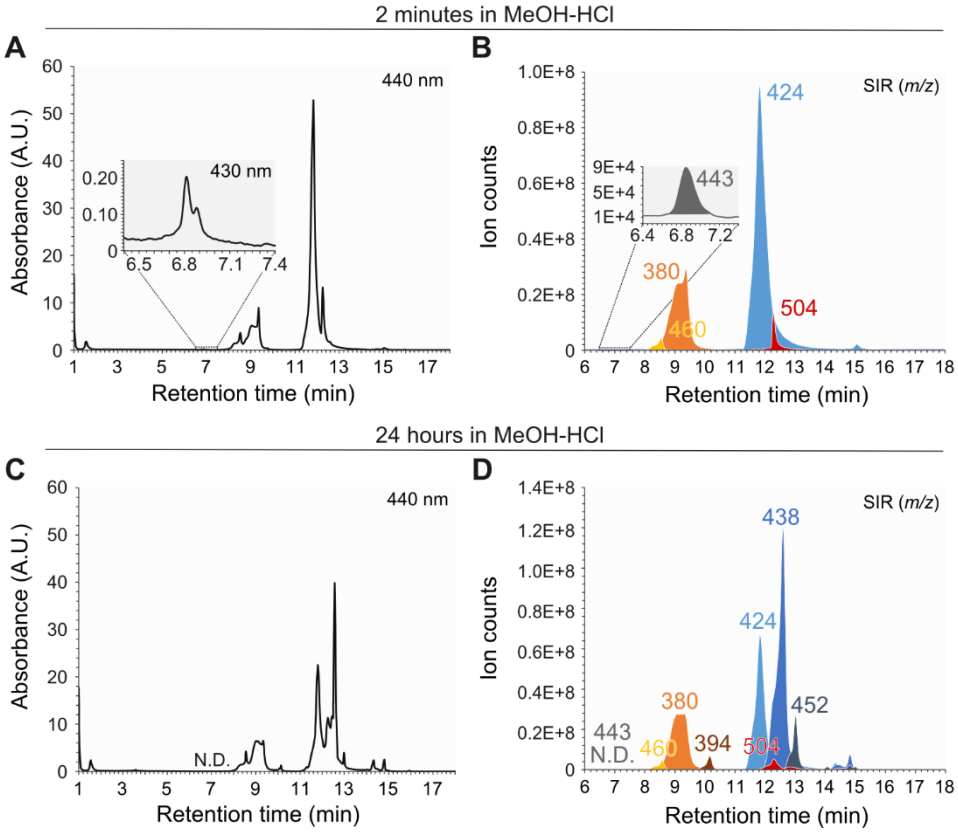

Fig. 1. **Chromatographic profiles of synthesized xanthommatin before and after storage in acidified methanol.** Xanthommatin was synthesized by oxidizing 3-hydroxykynurenine with potassium ferricyanide. **(A-B)** The ommatin solution was subjected to liquid chromatography (LC) two minutes after solubilisation in methanol acidified with 0.5 % HCl (MeOH-HCl). The eluted compounds were detected by their absorbance at 440 and 430 nm (A). The main molecular ions (electrospray ionization in positive mode) associated to each peak were monitored by a triple quadrupole mass spectrometer running in single ion reaction (SIR) mode (B). **(C-D)** The same ommatin solution was left for 24 hours at 20 °C in complete darkness. Compounds were separated by LC and detected using the same absorbance (A) and MS modalities (B) as described above.

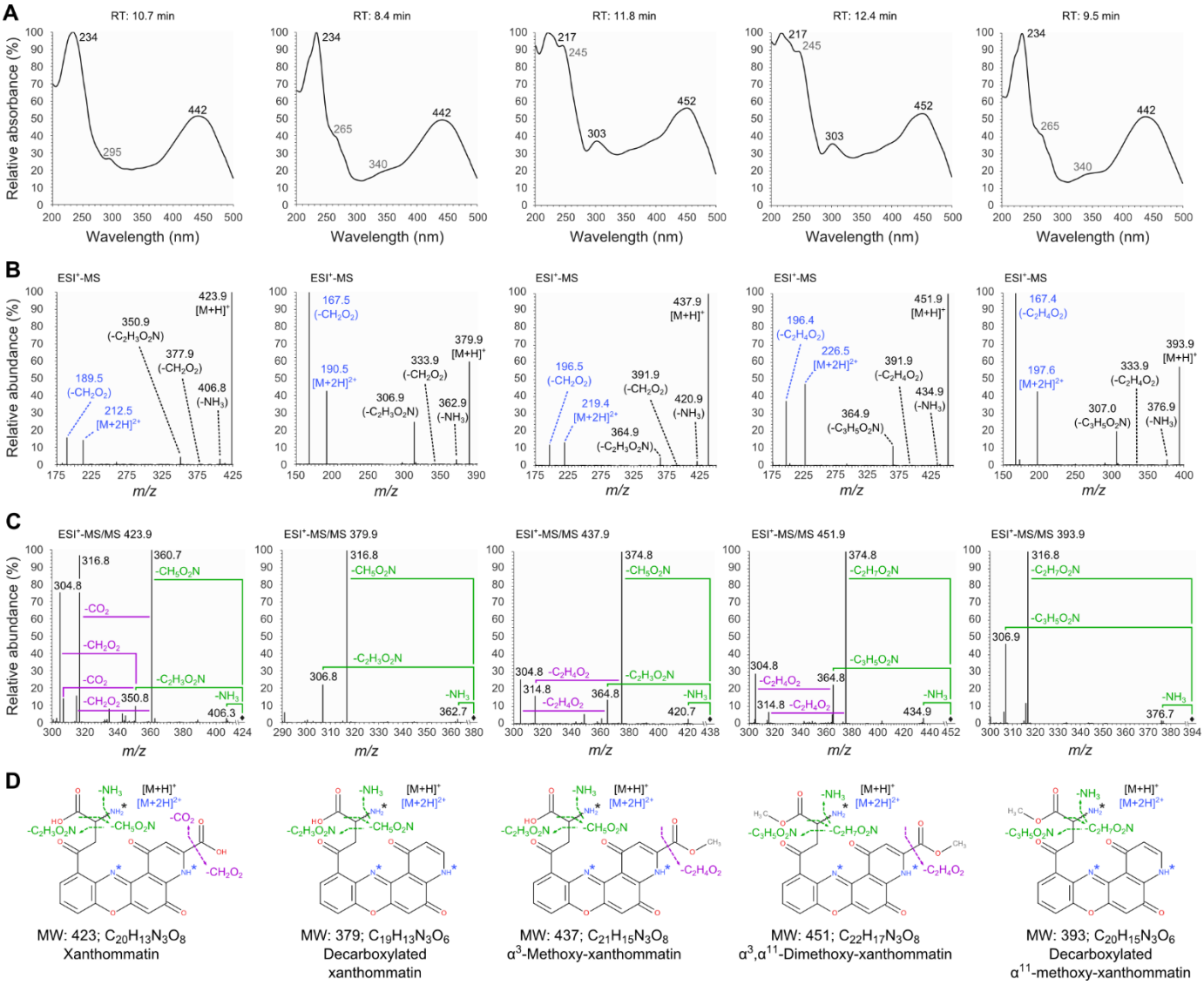

Figure 2. **Absorbance- and mass spectrometry-assisted elucidation of the structure of the five major ommatins detected after incubation in acidified methanol.** Ommatins incubated for 24 hours in acidified methanol were analysed by liquid chromatography coupled to a photodiode-array detector and a triple quadrupole mass spectrometer. **(A)** Absorbance spectra. For each metabolite, absorbance values were reported as percentages of the maximum absorbance value recorded in the range of 200 to 500 nm. Major and minor absorbance peaks are indicated in black and grey fonts, respectively. **(B)** Mass spectra showing molecular ions and in-source fragments. Black fonts, monocharged ions. Blue fonts, double-charged molecular ions. **(C)** Tandem mass (MS/MS) spectra of molecular ions obtained by collision-induced dissociation with argon. Black diamonds, $[M+H]^+$ *m/z*. Green fonts, fragmentations of the amino-acid chain. Purple fonts, fragmentations of the pyridine ring are indicated. **(D)** Elucidated structures of the five ommatins. MS/MS fragmentations are reported in green and purple like in panel C. Black asterisk, main charged basic site. Blue asterisks, potential charged basic sites of the double-charged molecular ions.

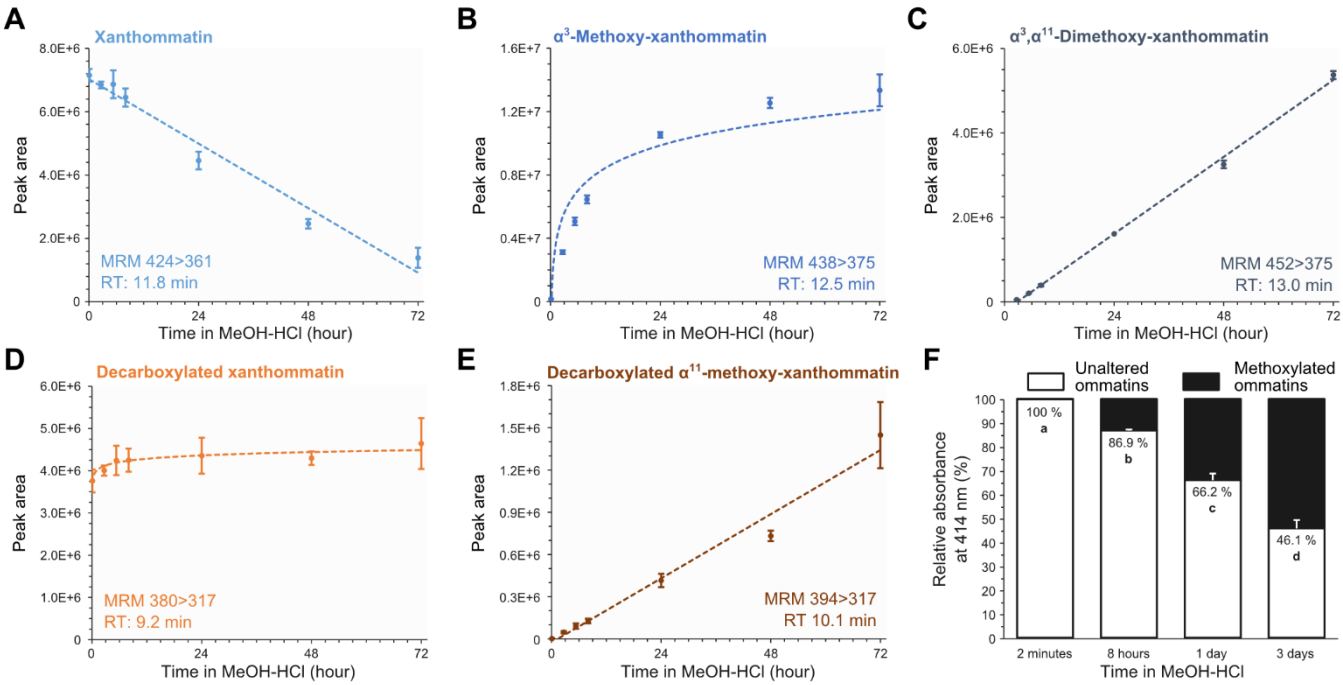

Figure 3. **Alterations of synthesized ommatins in acidified methanol at 20 °C in darkness.** Synthesized ommatins were solubilized in methanol acidified with 0.5 % HCl (MeOH-HCl) and stored for up to three days at 20 °C and in complete darkness. **(A-E)** Kinetics of alterations were followed by multiple reaction monitoring (MRM) mode of xanthommatin (A), α^3-methoxy-xanthommatin (B), α^3,α^{11}-dimethoxy-xanthommatin (C), decarboxylated xanthommatin (D) and decarboxylated α^{11}-xanthommatin (E). Values are mean ± SD of four to five samples. See Supplemental File S2 for information on regression analyses. **(F)** Relative quantifications of methoxylated ommatins compared to unaltered ones (i.e. xanthommatin and decarboxylated xanthommatin) were performed by measuring the absorbance of ommatins at 414 nm for each time point. Values are mean ± SE of five samples. Different letters indicate statistical differences (Kruskal-Wallis rank sum test: $\chi^2 = 17.857$, df = 3, p-value = 0.00047; pairwise comparisons using Wilcoxon rank sum test and Holm adjustment: p-values < 0.05).

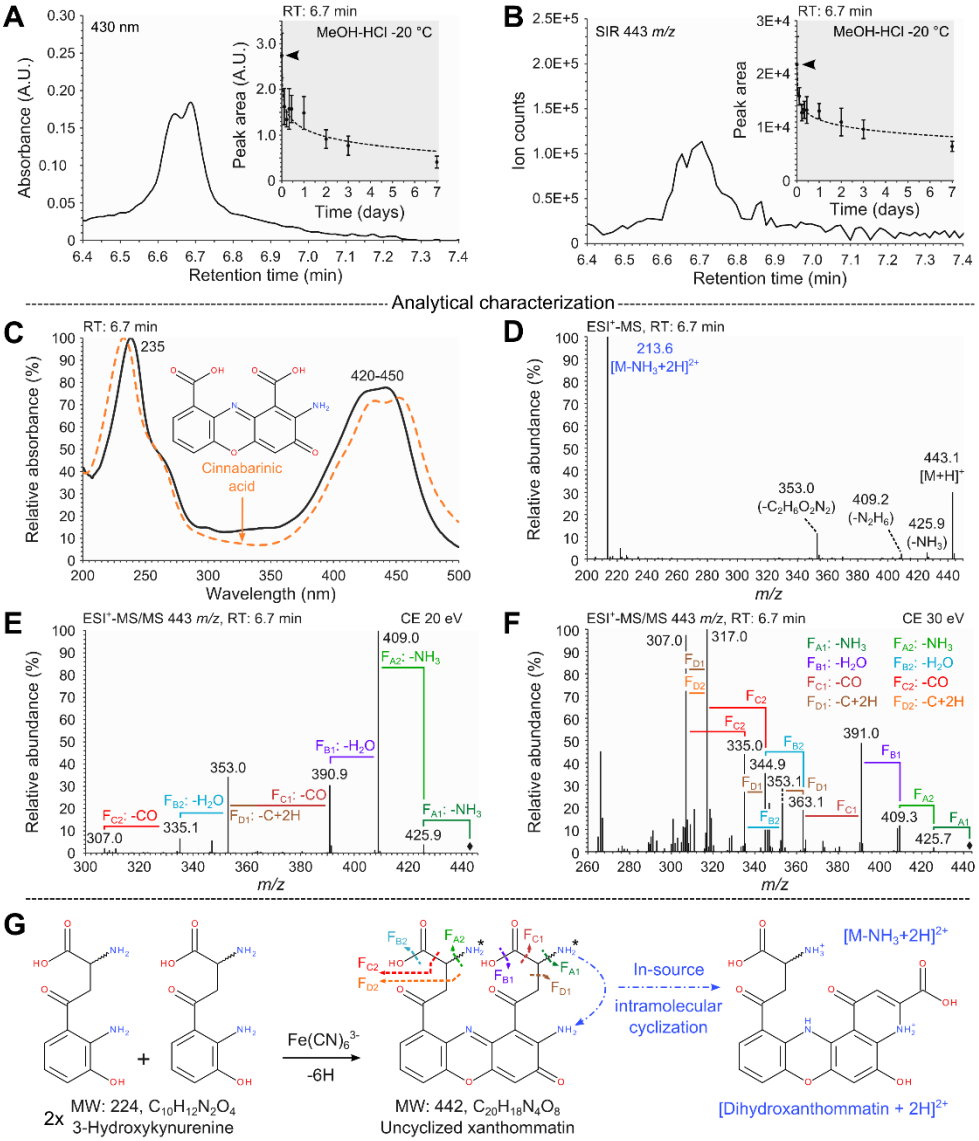

Figure 4. **Structural elucidation of uncyclized xanthommatin, the labile intermediate in the synthesis of xanthommatin. (A-B)** Chromatographic peaks (absorbance at 430 nm [A] and $[M+H]^+$ 443 m/z recorded in single ion reaction [SIR] mode [B]) corresponding to the labile ommatin-like compound detected in in vitro synthesis of xanthommatin by the oxidation of 3-hydroxkynurenine with $Fe(CN)_6^{3-}$. Insets show the decay of chromatographic peaks during storage in methanol acidified with 0.5 % HCl at -20 °C in darkness. Values are mean ± SD of five samples. See Supplemental File S2 for information on regression analysis. **(C)** Absorbance spectra. Solid line, labile ommatin-like compound. Dashed line, the aminophenoxazinone cinnabarinic acid. **(D)** Mass spectrum showing molecular ions and in-source fragments. Black fonts, monocharged ions. Blue font, double-charged ion. **(E-F)** Tandem mass spectra of the molecular ion obtained by collision-induced dissociation with argon at collision energies of 20 eV (E) and 30 eV (F). Fragmentations were classified in four types (F1 to F4) that occurred twice (FA and FB). Black diamonds, $[M+H]^+$ *m/z*. **(G)** Evidence for the structural elucidation of uncyclized xanthommatin. Colors of the MS/MS fragmentation pattern correspond to those in panels D-F. Black asterisks, potential charged basic sites.

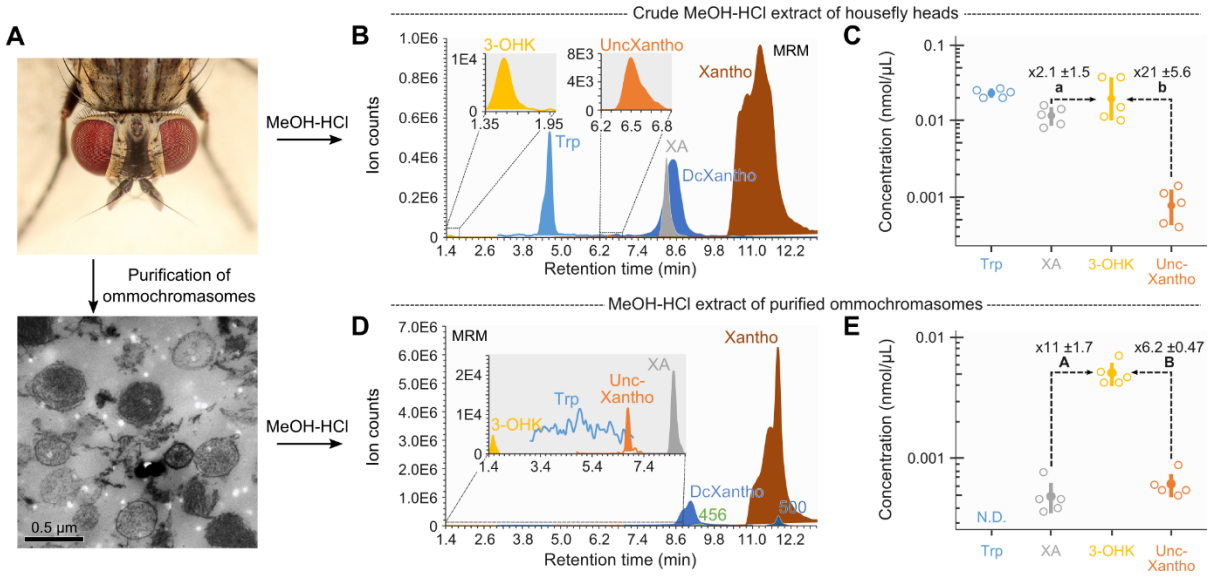

Figure 5. ***In vivo*** **localization of uncyclized xanthommatin and tryptophan→ommochrome metabolites from housefly eyes. (A)** Overview of the purification and extraction protocols of ommochromes from housefly eyes. **(B)** Chromatographic profile in Multiple Reaction Monitoring (MRM) mode of the six main metabolites of the tryptophan→ommochrome pathway detected in acidified methanol (MeOH-HCl) extracts of housefly eyes (crude extracts). DcXantho, decarboxylated xanthommatin, 3-OHK, 3-hydroxykynurenine, Trp, tryptophan, UncXantho, uncyclized xanthommatin. Xantho, xanthommatin. XA, xanthurenic acid. **(C)** Five µL of crude extract were injected in the chromatographic system and absolute quantifications of tryptophan, xanthurenic acid, 3-hydroxykynurenine and uncyclized xanthommatin were performed based on available standards (uncyclized xanthommatin levels are expressed as cinnabarinic acid equivalents). Open circles, measures of five independent extracts. Filled circles and error bars, means ± SD of five samples. Ratios of 3-hydroxykynurenine to xanthurenic acid and to uncyclized xanthommatin are shown (mean ± SD, N = 5). **(D-E)** Same as panels B (D) and C (E) but for MeOH-HCl extracts of purified ommochromasomes from housefly eyes. The tryptophan signal was below the signal-to-noise ratio. Statistical differences (p-value < 0.05) between ratios within panels (paired *t*-test) and between panels (unpaired *t*-test) are indicated by different letters and capitals, respectively. N.D., not detected. See Supplemental File S2 for information on statistical analyses. Photograph credits: (A) Sanjay Acharya (CC BY SA).

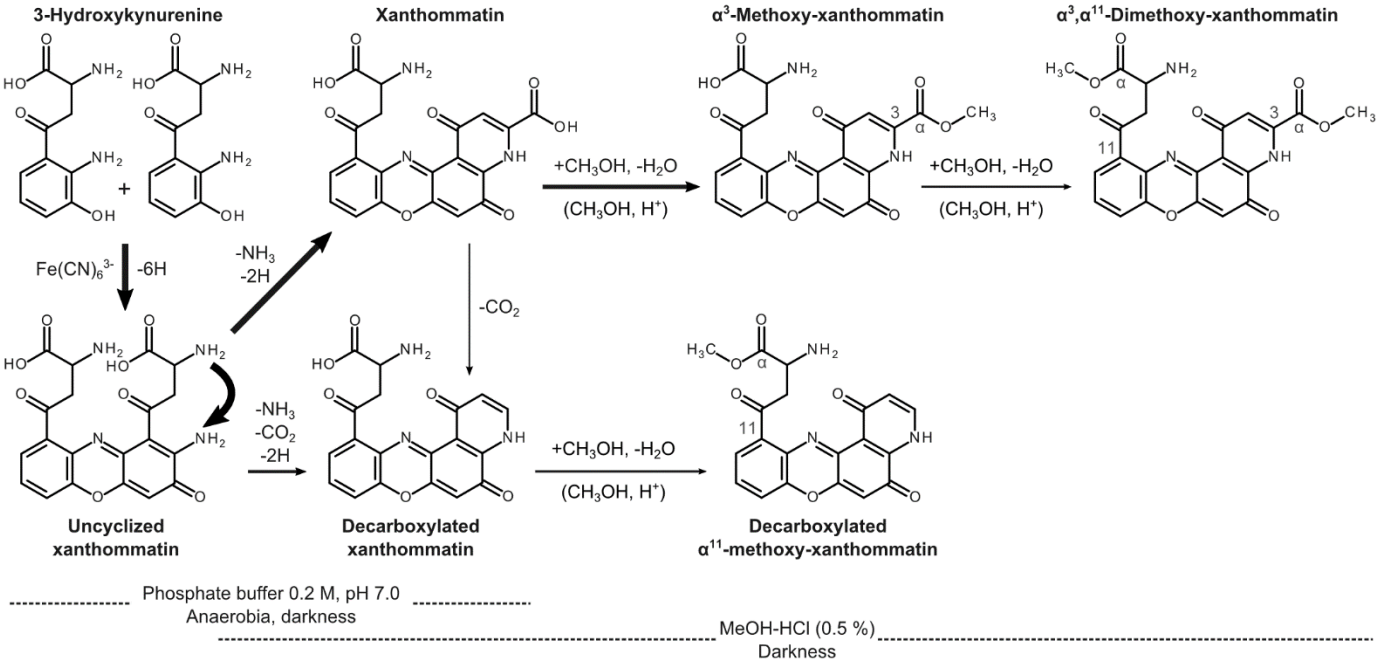

Scheme 2. ***In vitro* formation and alteration of ommatins.** Ommatins were synthesized by the oxidative condensation of 3-hydroxykynurenine in presence of potassium ferricyanide. Oxidative condensation of *ortho*-aminophenols proceeds through the loss of six electrons, leading to the formation of an aminophenoxazinone, here uncyclized xanthommatin. Uncyclized xanthommatin then rapidly undergoes intramolecular cyclization and oxidation, forming the two pyrido[3,2-*a*]phenoxazinone xanthommatin and decarboxylated xanthommatin. Decarboxylated xanthommatin could also be produced from the direct decarboxylation of xanthommatin. When solubilized in acidified methanol, ommatins readily undergo thermal additions of methanol, which leads to their methoxylation. Methoxylations primarily affect the carboxylic acid of the pyridine ring (at position α^3), if present, and secondarily the amino-acid chain (at position α^{11}). In acidified methanol, uncyclized xanthommatin also decays by intramolecular cyclization and xanthommatin slowly decarboxylates. Relative sizes of arrows are indicative of reaction rates.

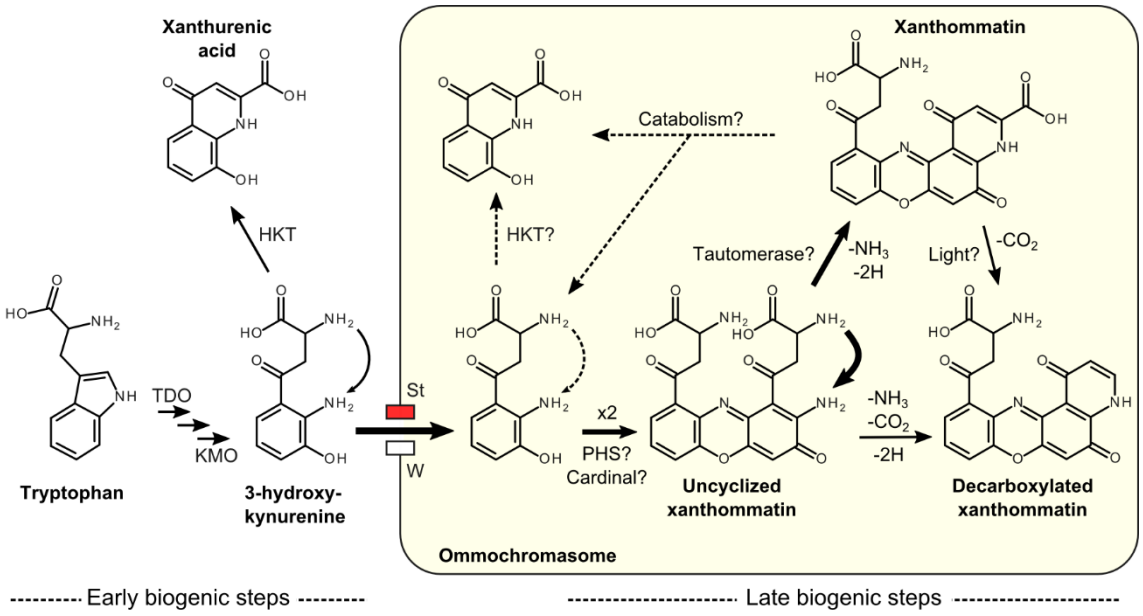

Scheme 3. **Proposed biosynthetic pathway of ommatins through the formation of uncyclized xanthommatin in the housefly eye.** The three early biogenic steps of ommatins involve the oxidation of tryptophan into 3-hydroxykynurenines. The two corresponding major enzymes are the cytosolic tryptophan 2,3-dioxygenase (TDO) and the mitochondrial kynurenine 3-monooxygenase (KMO). Any of these three early steps could be performed by other cells than pigmented ones. 3-Hydroxykynurenine is then transported through the membrane of ommochromasomes by scarlet (St) and white (W) ABC transporters. In ommochromasomes, ommatins are produced and modified during the late biogenic steps of the tryptophan→ommochrome pathway. First, the oxidative dimerization of two 3-hydroxykynurenines produces the labile intermediate uncyclized xanthommatin. Second, uncyclized xanthommatin rapidly undergoes intramolecular cyclization and rearrangement to form xanthommatin. The formation of uncyclized xanthommatin might either be spontaneous, catalyzed by an unspecific unknown phenoxazinone synthase (PHS) or by the heme peroxidase Cardinal. Decarboxylation of the pyridine ring of xanthommatin could happen either concomitantly to the rearrangement of protons or after xanthommatin formation. A tautomerase might act after the pyridine ring closure of uncyclized xanthommatin to favor the formation of xanthommatin over its decarboxylated form. The direct decarboxylation of xanthommatin could also happened in a water-based environment, possibly by the action of light on xanthommatin. Outside ommochromasomes, xanthurenic acid is formed by the transamination of 3-hydroxykynurenine, a reaction catalyzed by the 3-hydroxykynurenine transaminase (HKT). Within ommochromasomes, traces of xanthurenic acid could result from the transamination of 3-hydroxykynurenine or from the degradation of xanthommatin. Relative sizes of arrows are indicative of reaction rates.